

재료상변태

Phase Transformation of Materials

2008. 11. 18.

박은수

서울대학교 재료공학

Contents for previous class

“Alloy solidification”

- Solidification of single-phase alloys

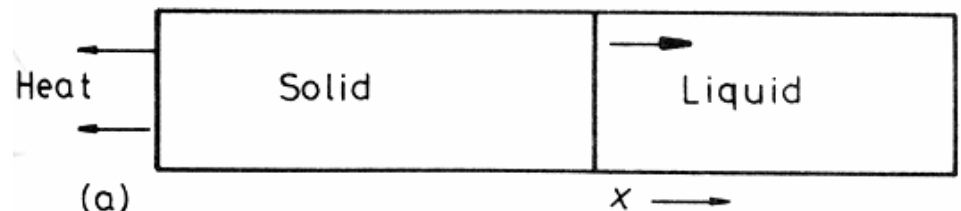
- Three limiting cases

1) Equilibrium Solidification

2) No Diffusion in Solid, Perfect Mixing in Liquid

3) No Diffusion on Solid, Diffusional Mixing in the Liquid

Planar S/L interface
→ **unidirectional solidification**



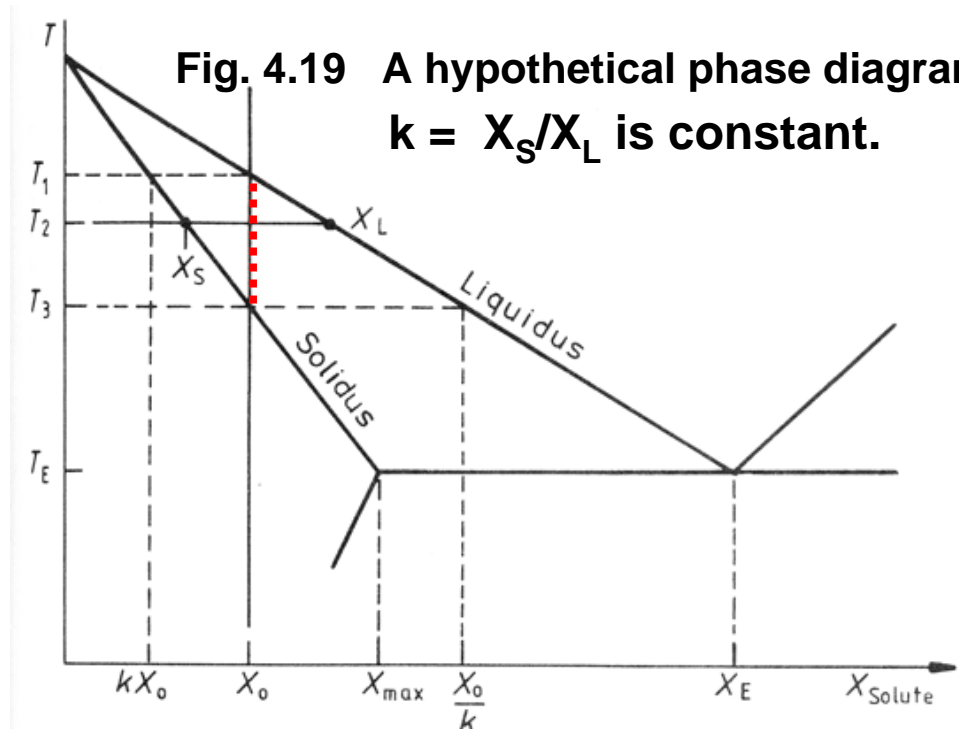
1) Equilibrium Solidification Low cooling rate

$$k = \frac{X_S}{X_L} < 1$$

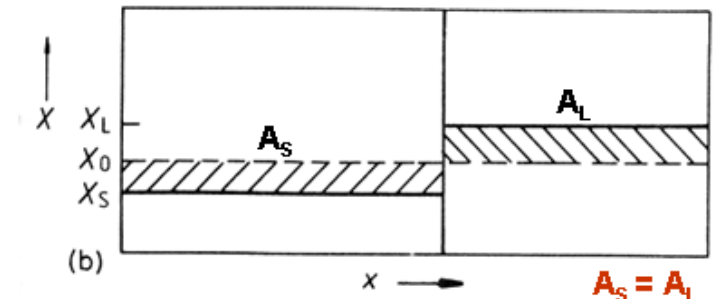
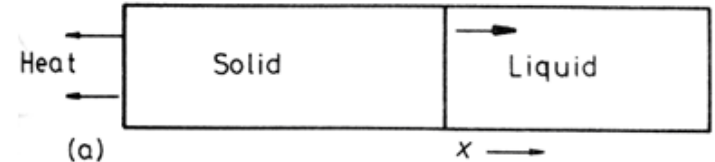
k : partition coefficient

X : mole fraction of solute

In this phase diagram of **straight solidus and liquidus**, k is independent of T .



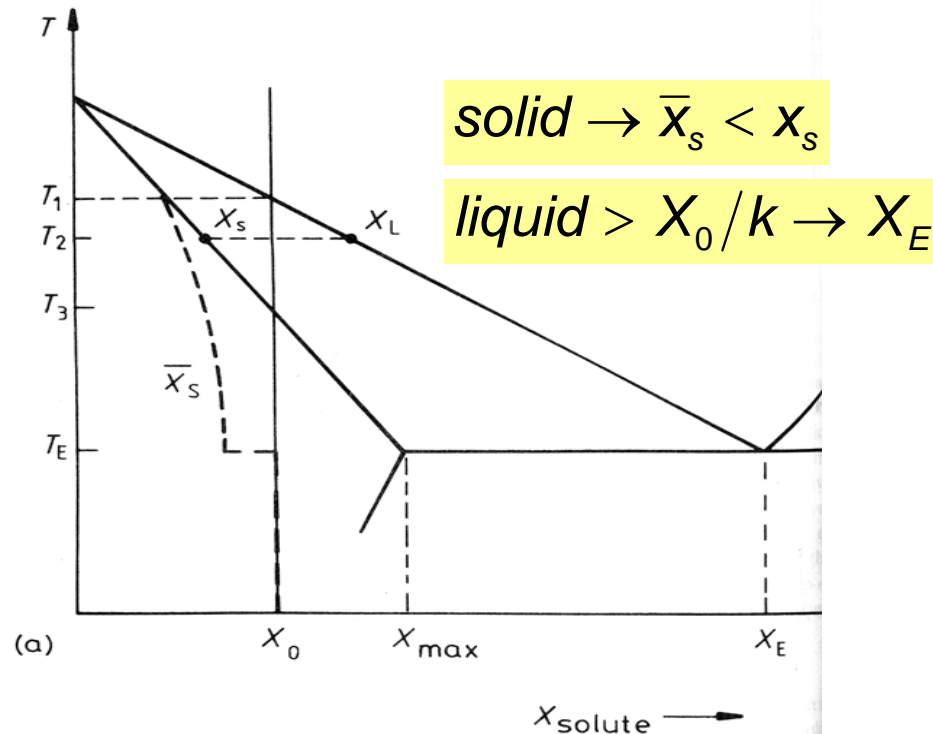
- **Sufficient time for diffusion in solid & liquid**
- Relative amount of solid and liquid : **lever rule**
- Solidification starts at T_1 ($X_S = kX_0$) and ends at T_3 ($X_L = X_0/k$).



2) No Diffusion in Solid, Perfect Mixing in Liquid

: high cooling rate, efficient stirring

- Separate layers of solid retain their original compositions
- mean comp. of the solid (\bar{X}_s) $<$ X_s
- Liquid become richer than $X_0/K \rightarrow X_E$
- Variation of X_s : solute rejected to the liquid



local equil. at S/L interface

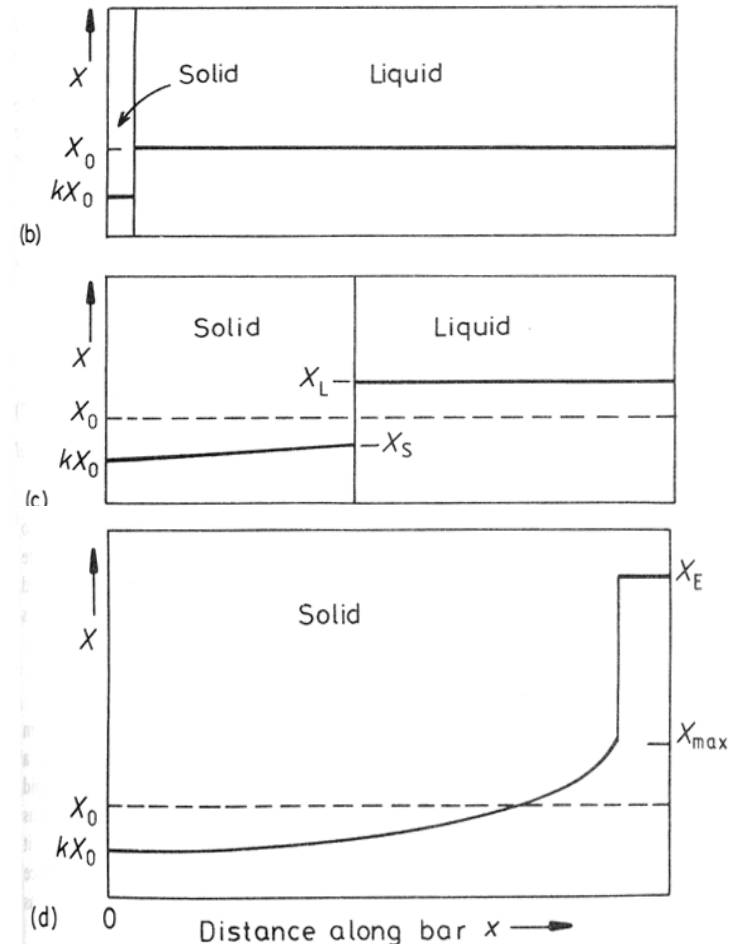


Fig. 4.21 Planar front solidification of alloy X_0 in fig. 4.19 assuming no diffusion in the solid, but complete mixing in the liquid. (a) As Fig. 4.19, but including the mean composition of the solid. (b) Composition profile just under T_1 . (c) Composition profile at T_2 (compare with the profile and fraction solidified in Fig.4.20b) (d) Composition profile **at the eutectic temperature and below.**

3) No Diffusion on Solid, Diffusional Mixing in the Liquid

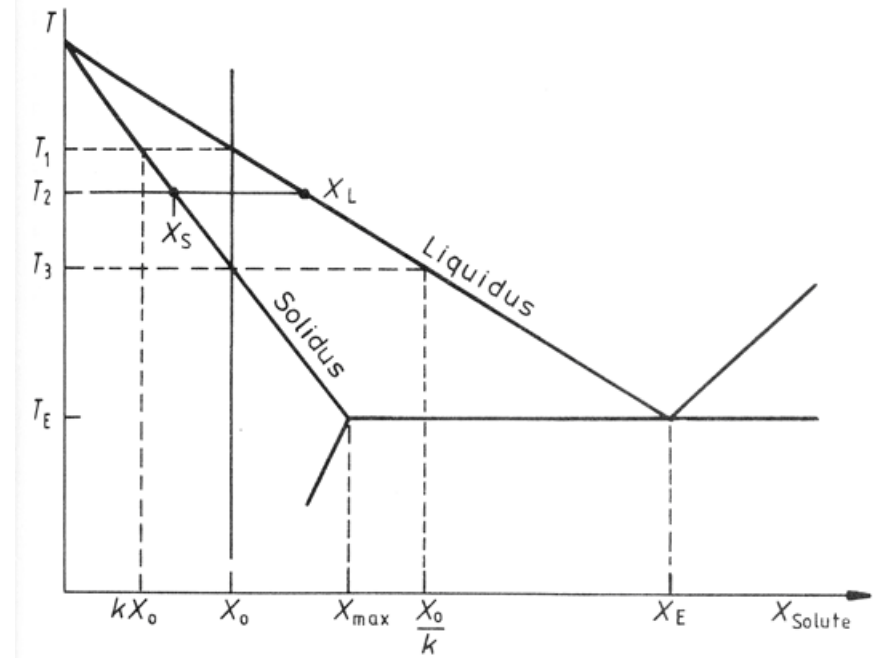
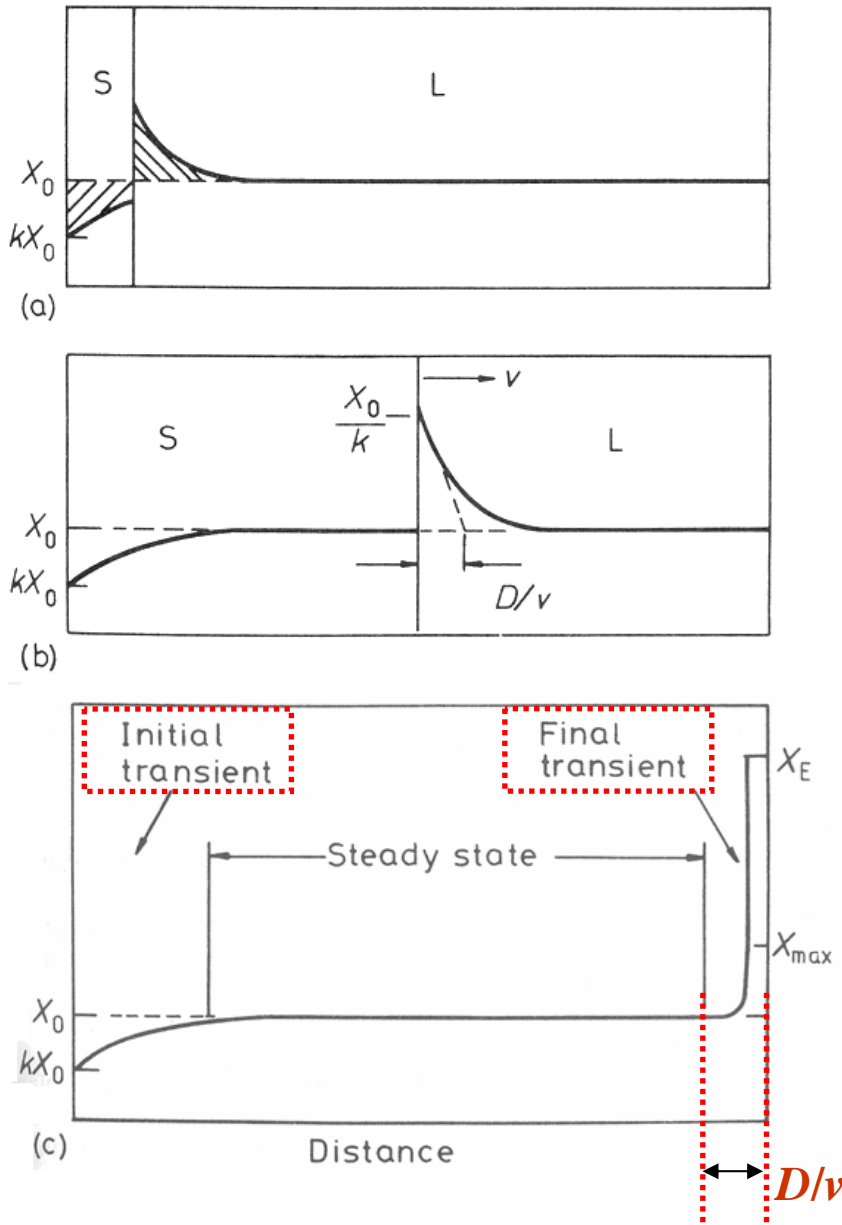
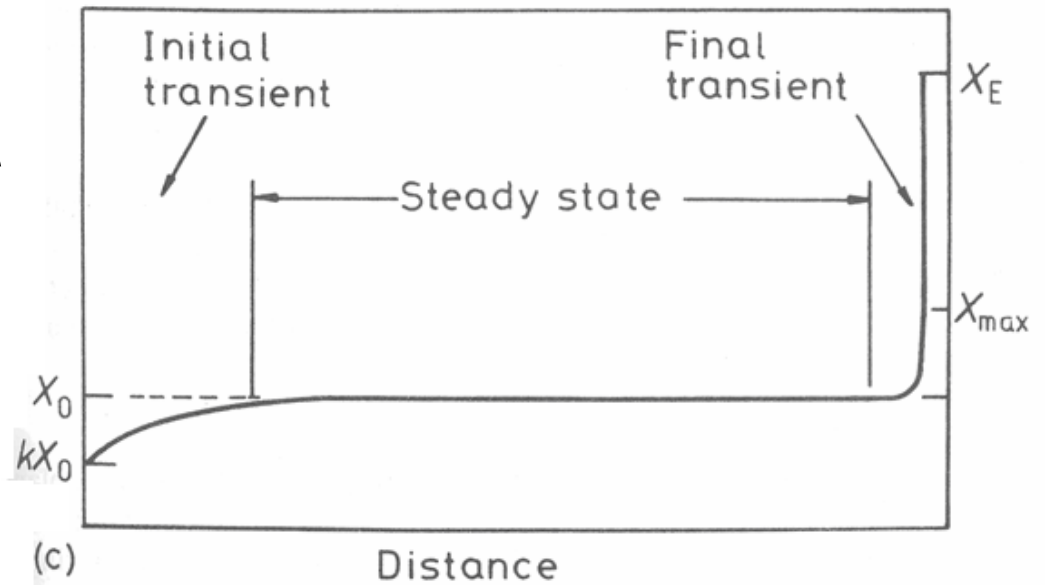
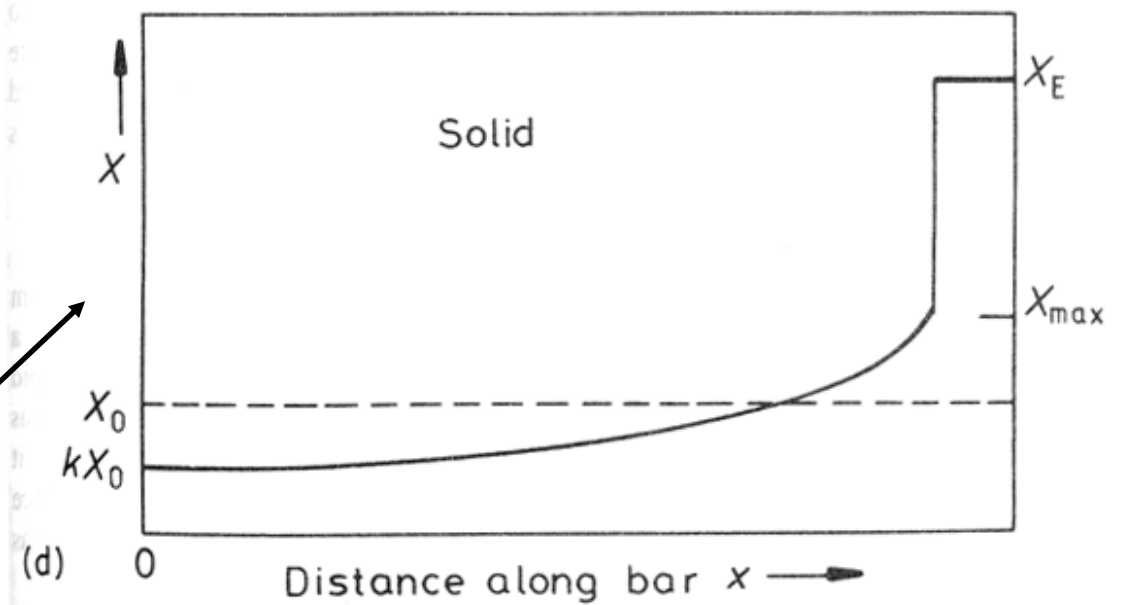


Fig. 4.22 Planar front solidification of alloy X_0 in Fig. 4.19 assuming no diffusion in solid and no stirring in the liquid.

- (a) Composition profile when S/L temperature is between T_2 and T_3 in Fig. 4.19.
- (b) Steady-state at T_3 . The composition solidifying equals the composition of liquid far ahead of the solid (X_0).
- (c) Composition profile at T_E and below, showing the final transient.

실제의 농도분포
두 가지 경우의 중간형태



➡ Zone Refining

Contents for today's class

4.3 Alloy solidification

- Solidification of single-phase alloys
- Eutectic solidification
- Off-eutectic alloys
- Peritectic solidification

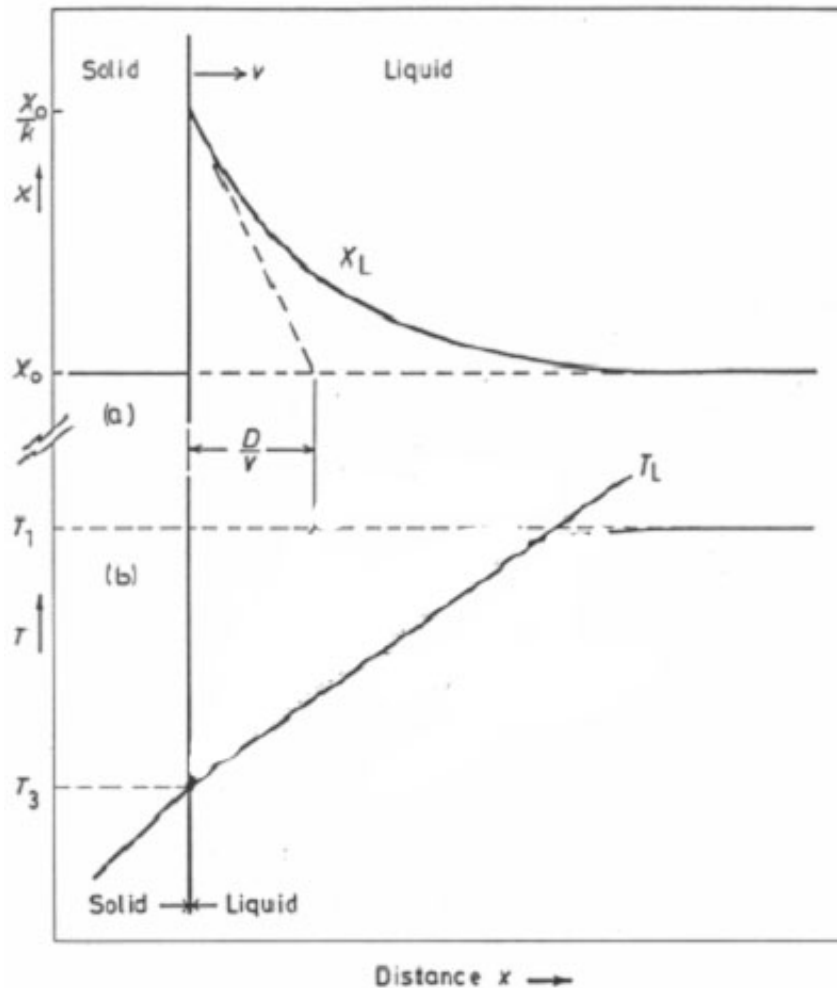
4.4 Solidification of ingots and castings

- Ingot structure
- Segregation in ingot and castings
- Continuous casting

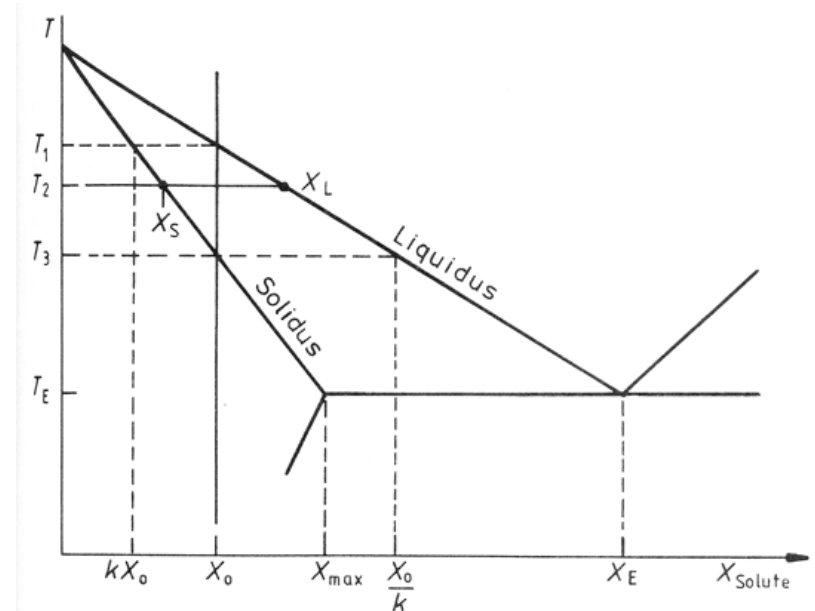
Cellular and Dendritic Solidification

Fast Solute diffusion similar to the **conduction of latent heat** in pure metal, possible to break up the planar front into dendrites.

→ complicated by the **possible temp. gradient** in the liquid.



What would be T_e along the concentration profile ahead of the growth front during steady-state solidification?



Constitutional Supercooling

Condition for a stable planar interface

$$T_L' > (T_1 - T_3) / (D/v)$$

$$T_L' / v > (T_1 - T_3) / D$$

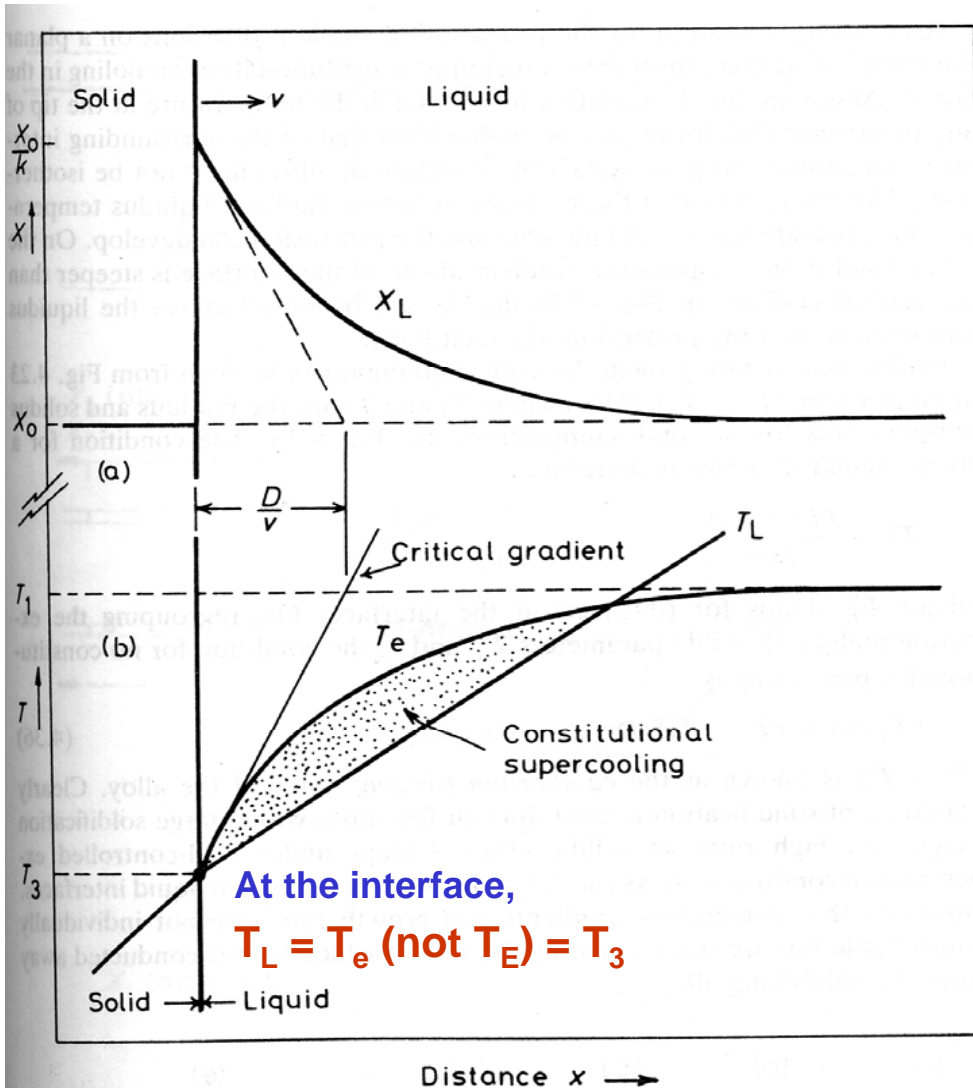


Fig. 4.23 The origin of constitutional supercooling ahead of a planar solidification front. (a) Composition profile across the solid/liquid interface during steady-state solidification. The dashed line shows dX_L/dx at the S/L interface. (b) The temperature of the liquid ahead of the solidification front follows line T_L . The equilibrium liquidus temperature for the liquid adjacent to the interface varies as T_e . Constitutional supercooling arises when T_L lies under the critical gradient.

Cellular and Dendritic Solidification

- **Constitutional supercooling :**

At the interface, $T_L = T_e$ (not T_E) = T_3 .

- **Criterion for the planar interface :**

$T_L' / \nu > (T_1 - T_3) / D$: the protrusion melts back. 조성적 과냉 X

($T_1 - T_3$: Equilibrium freezing range of alloy)

→ **Large range of $T_1 - T_3$ or high ν promotes protrusions.**

- **Dendrites**

Solute effect : low k enlarges $T_1 - T_3$ promotes dendrites.

→ Development of secondary arms and tertiary arms: $\langle 100 \rangle$

Cooling rate effect : Fast cooling makes lateral diffusion of the rejected solutes difficult and promotes cell formation of smaller cell spacing.

Cellular Solidification

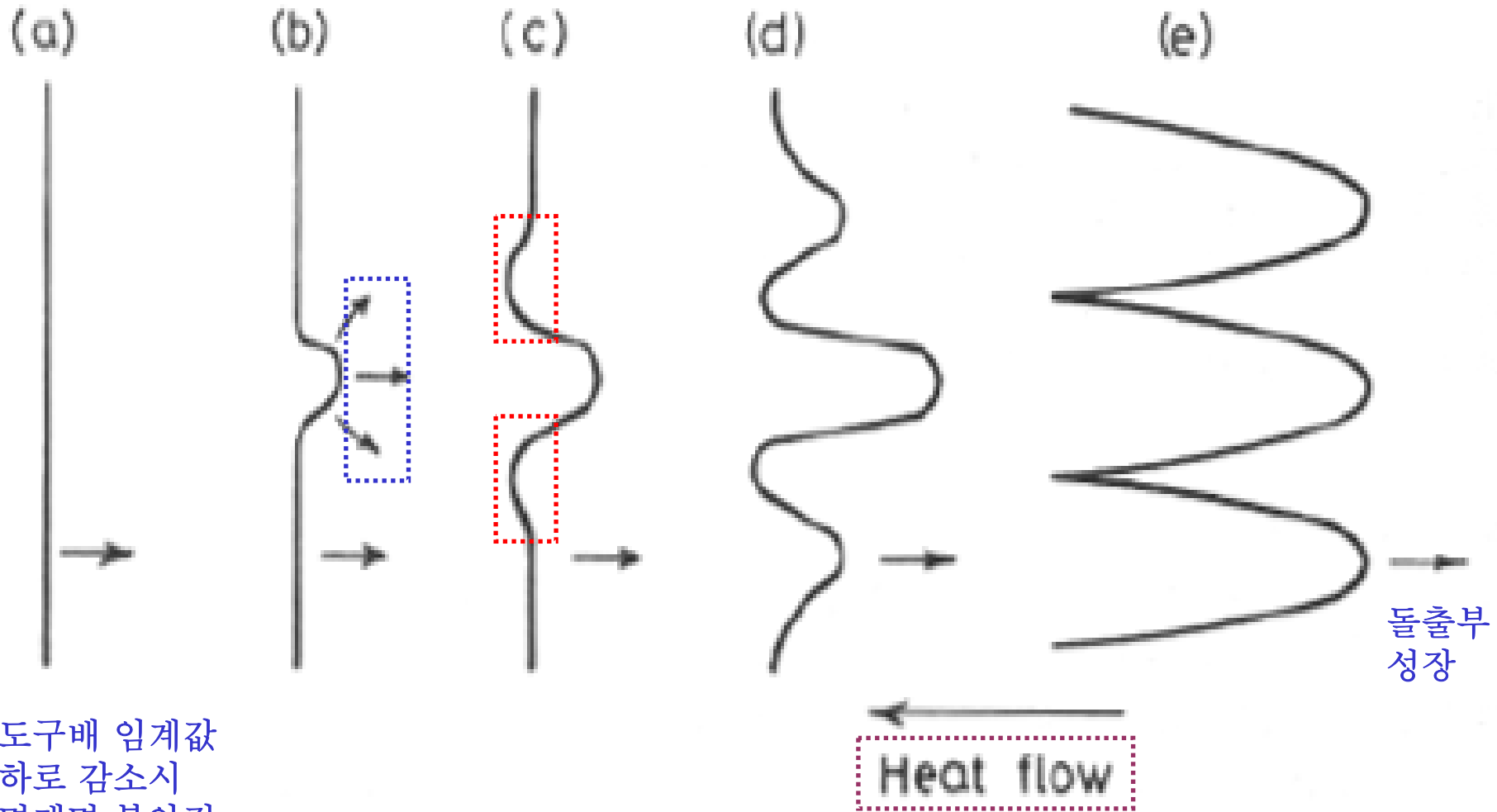
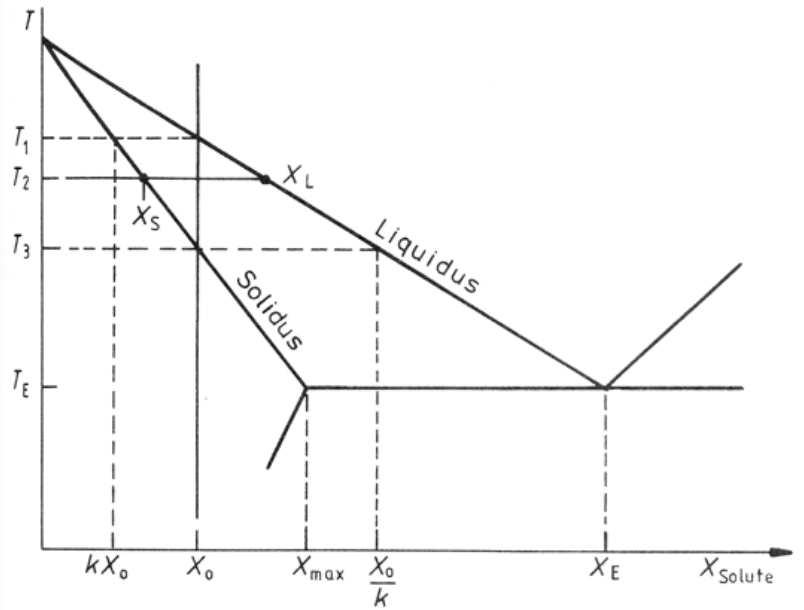
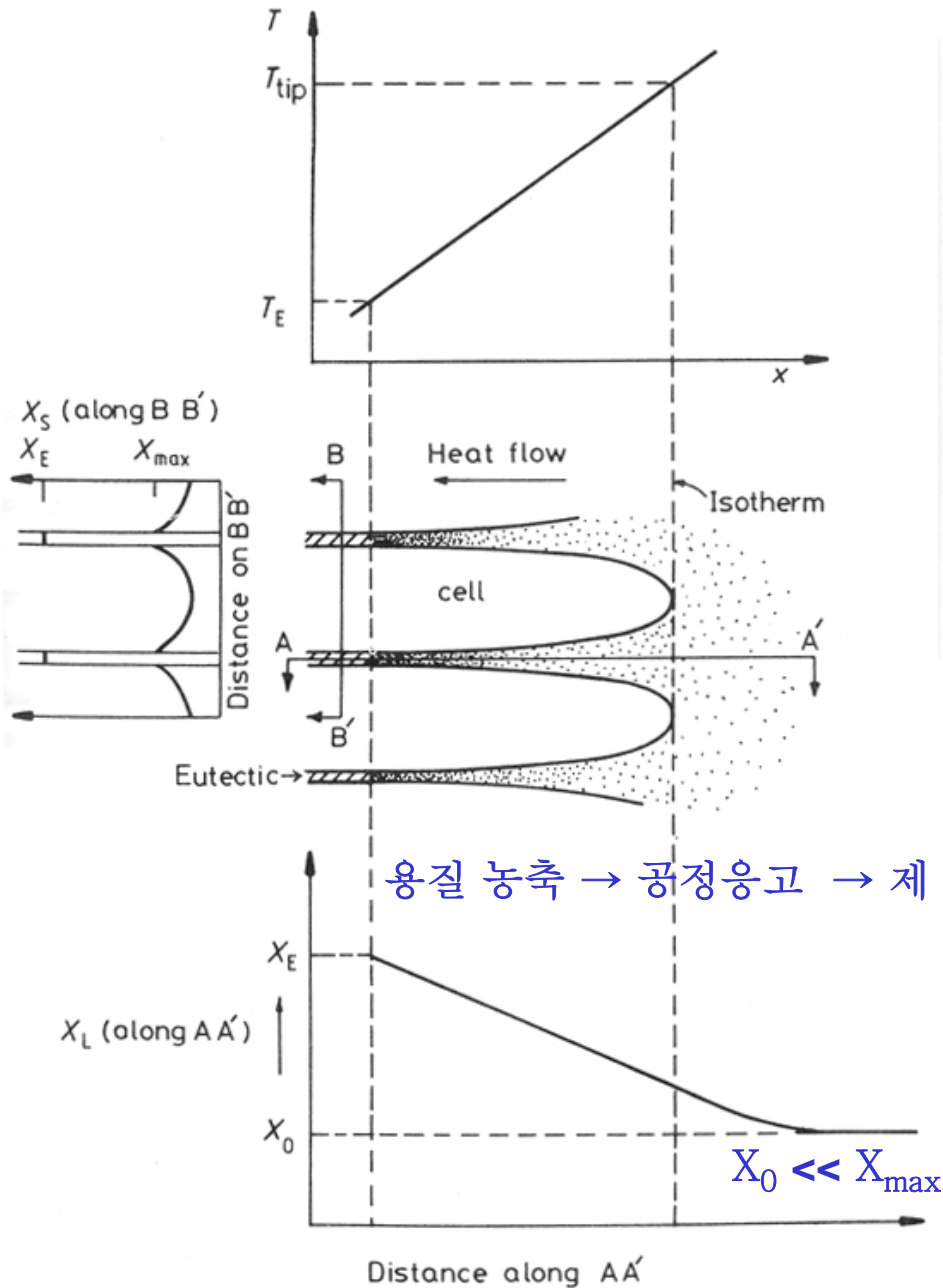


Fig. 4.24 The breakdown of an initially planar solidification front into cells



용질 농축 → 공정응고 → 제 2 상 형성

Fig. 4.25 Temperature and solute distributions associated with cellular solidification.

Note that solute enrichment in the liquid between the cells, and coring in the cells with eutectic in the cell walls.

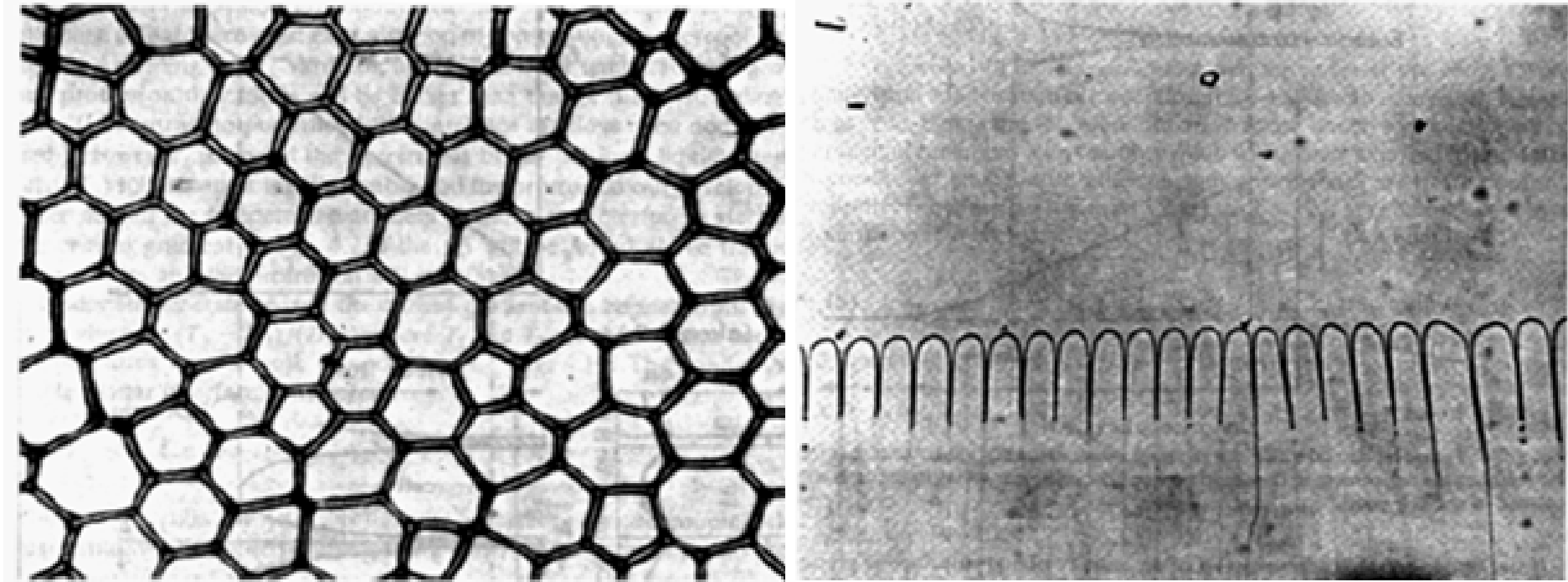


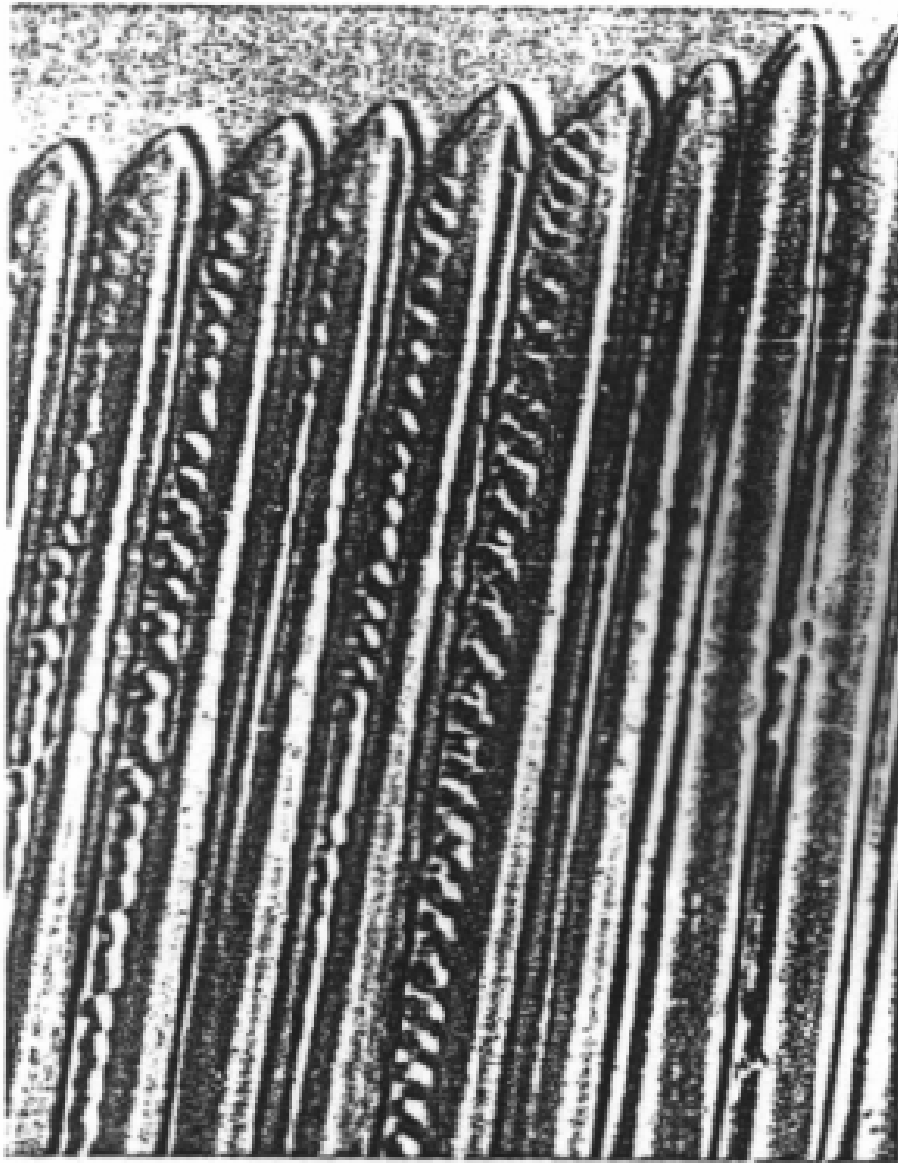
Fig. 4.26 Cellular microstructures.

(a) A decanted interface of a cellularly solidified Pb-Sn alloy ($\times 120$)

(after J.W. Rutter in *Liquid Metals and Solidification*, American Society for Metals, 1958, p. 243).

(b) Longitudinal view of cells in carbon tetrabromide ($\times 100$)

(after K.A. Jackson and J.D. Hunt, *Acta Metallurgica* 13 (1965) 1212).



형태 변화

세포상 조직과

온도구배가

특정한 범위로

유지될 때 안정

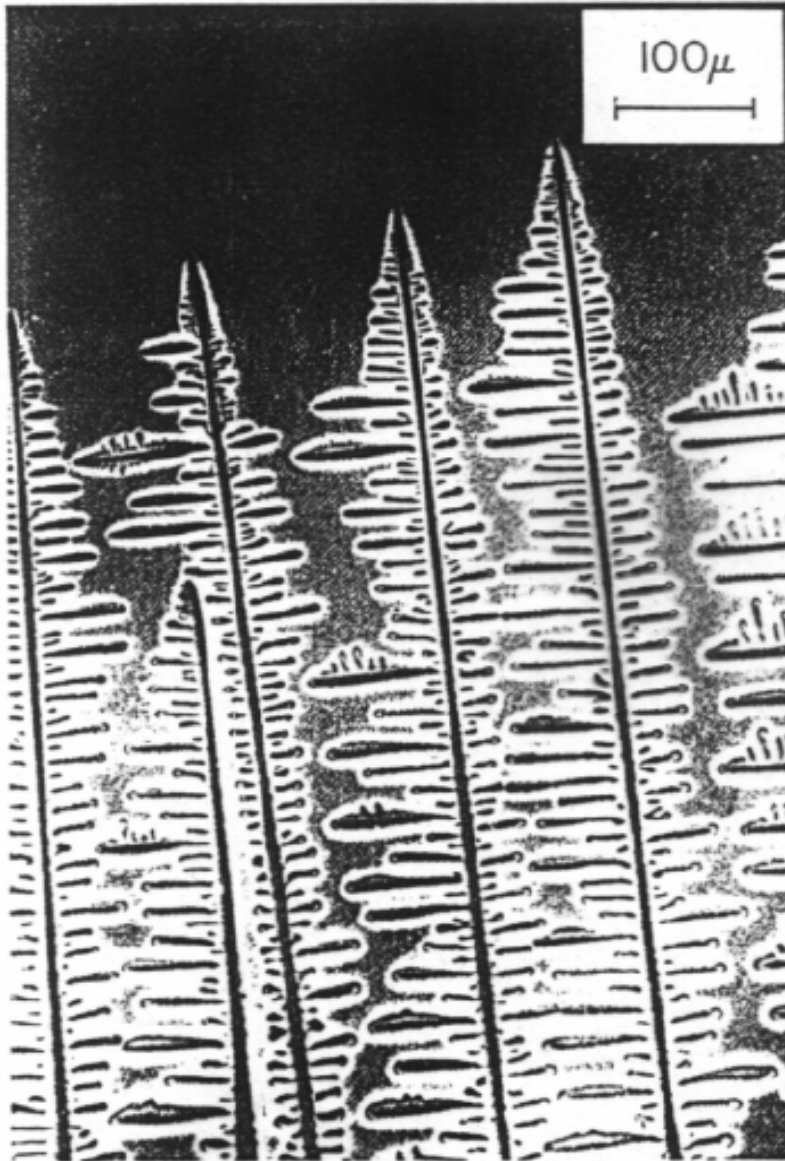
수지상 조직의 천이

온도구배 ↓ 면

수지상 형성

Fig. 4.27 Cellular dendrites in carbon tetrabromide.

(After L.R. Morris and W.C. Winegard, Journal of Crystal Growth 6 (1969) 61.)



1차 가지 성장 방향 변화

열전도 방향 → 결정학적 우선 방향

Fig. 4.28 Columnar dendrites in a transparent organic alloy.
(After K.A. Jackson in *Solidification*, American Society for Metals, 1971, p. 121.)⁵

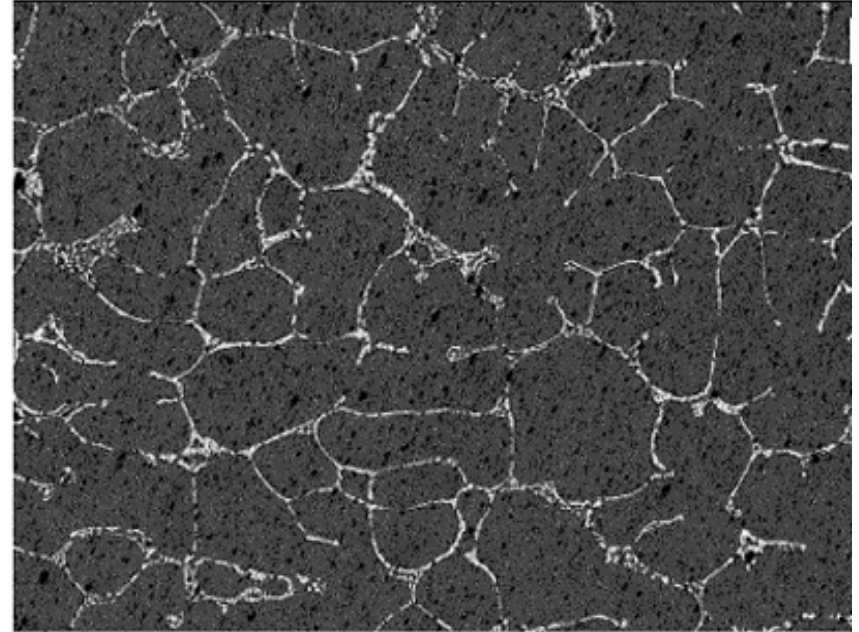
4.3.2 Eutectic Solidification

Normal eutectic



Fig. 4.30 Rod-like eutectic. Al_6Fe rods in Al matrix. Transverse section. Transmission electron micrograph (x 70000).

Anomalous eutectic



The microstructure of the **Pb-61.9%Sn (eutectic) alloy** presented a coupled growth of the (Pb)/bSn eutectic. There is a remarkable change in morphology increasing the degree of undercooling with transition from regular lamellar to **anomalous eutectic**.

4.3.2 Eutectic Solidification

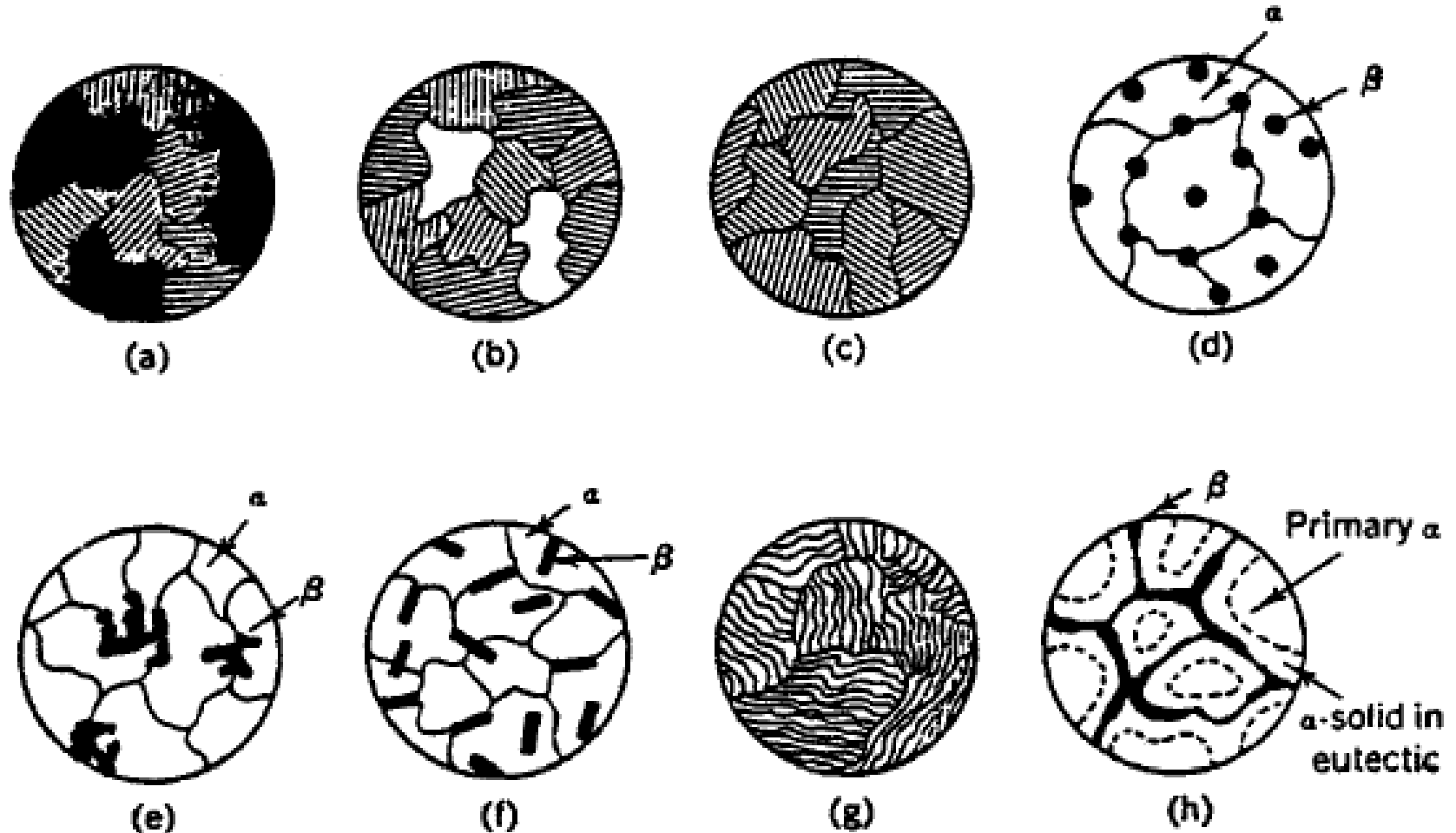
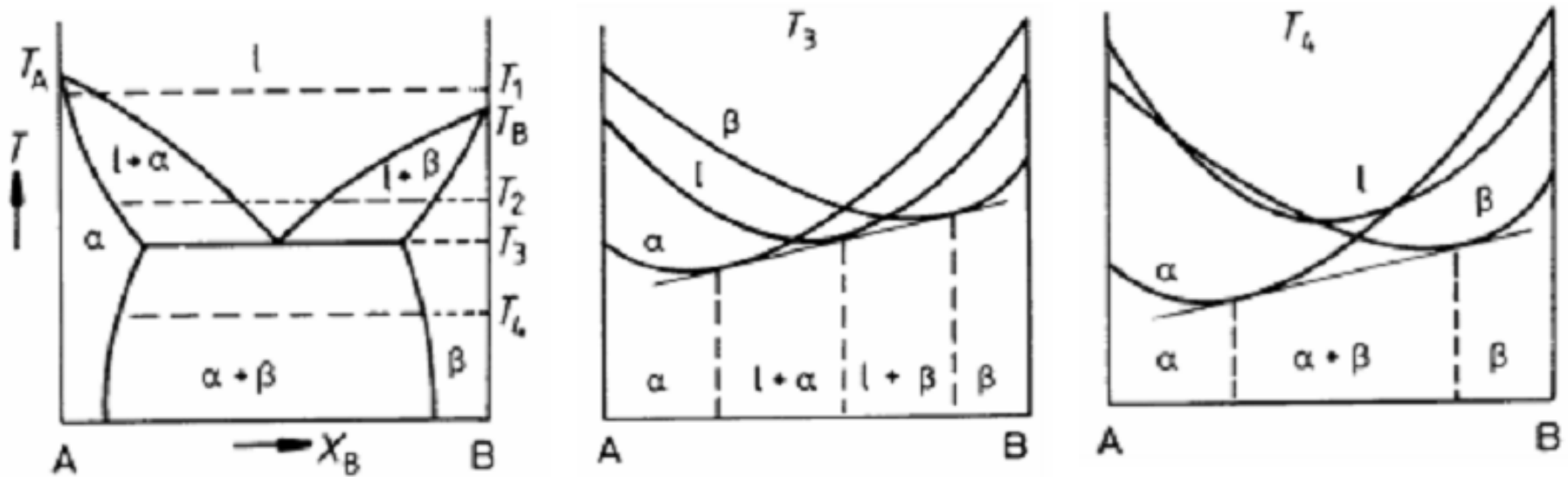


Fig. 14 Schematic representation possible in eutectic structures. (a), (b) and (c) are alloys shown in fig. 13; (d) nodular; (e) Chinese script; (f) acicular; (g) lamellar; and (h) divorced.

4.3.2 Eutectic Solidification (Thermodynamics)



Plot the diagram of Gibbs free energy vs. composition at T_3 and T_4 .

What is the driving force for the eutectic reaction ($L \rightarrow \alpha + \beta$) at T_4 at C_{eut} ?

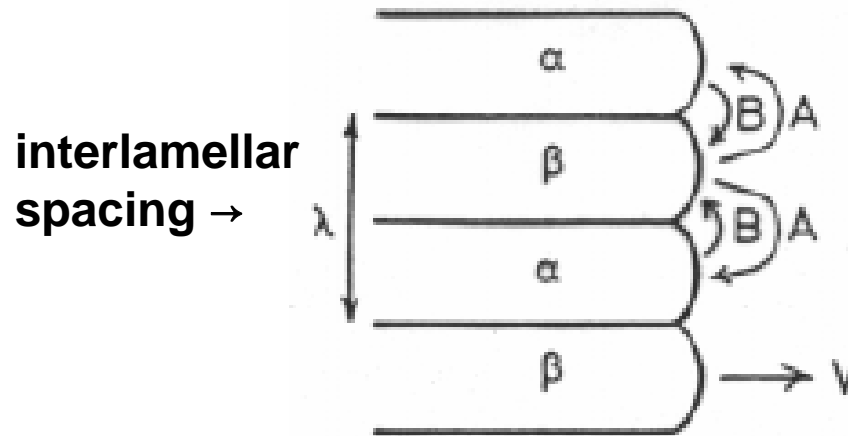
What is the driving force for nucleation of α and β ?

Eutectic Solidification (Kinetics)

If α is nucleated from liquid and starts to grow, what would be the composition at the interface of α/L determined?

→ rough interface & local equilibrium

How about at β/L ? Nature's choice?



What would be a role of the curvature at the tip?

→ Gibbs-Thomson Effect

Eutectic Solidification

How many α/β interfaces per unit length?

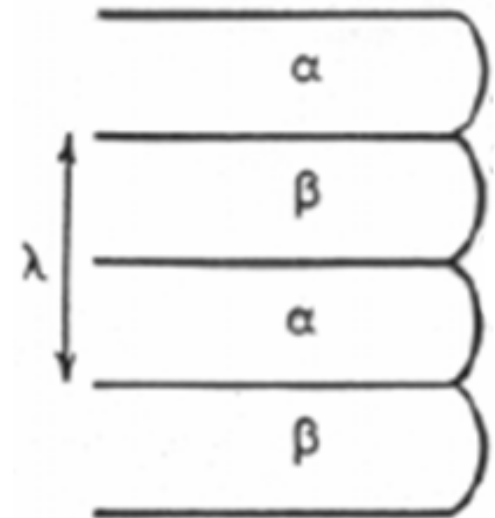
$$\rightarrow 1/\lambda \times 2$$

For an interlamellar spacing, λ , there is a total of $(2/\lambda)$ m² of α/β interface per m³ of eutectic.

$$\Delta G = \Delta\mu \cong \frac{L\Delta T}{T_m}$$

Driving force for nucleation

$$\rightarrow \Delta G = \Delta\mu = \frac{2\gamma}{\lambda} \times V_m$$



$$\lambda \rightarrow \infty, \quad \Delta G(\infty) = \Delta\mu = \frac{\Delta H \Delta T_0}{T_E}$$

$$\Delta G(\lambda) = ? = -\Delta G(\infty) + \frac{2\gamma V_m}{\lambda}$$

What would be the minimum λ ?

Critical spacing, $\lambda^* : \Delta G(\lambda^*) = 0$

$$\Delta G(\infty) = \frac{2\gamma V_m}{\lambda^*}$$

$$\lambda^* = -\frac{2T_E \gamma V_m}{\Delta H \Delta T_0}$$

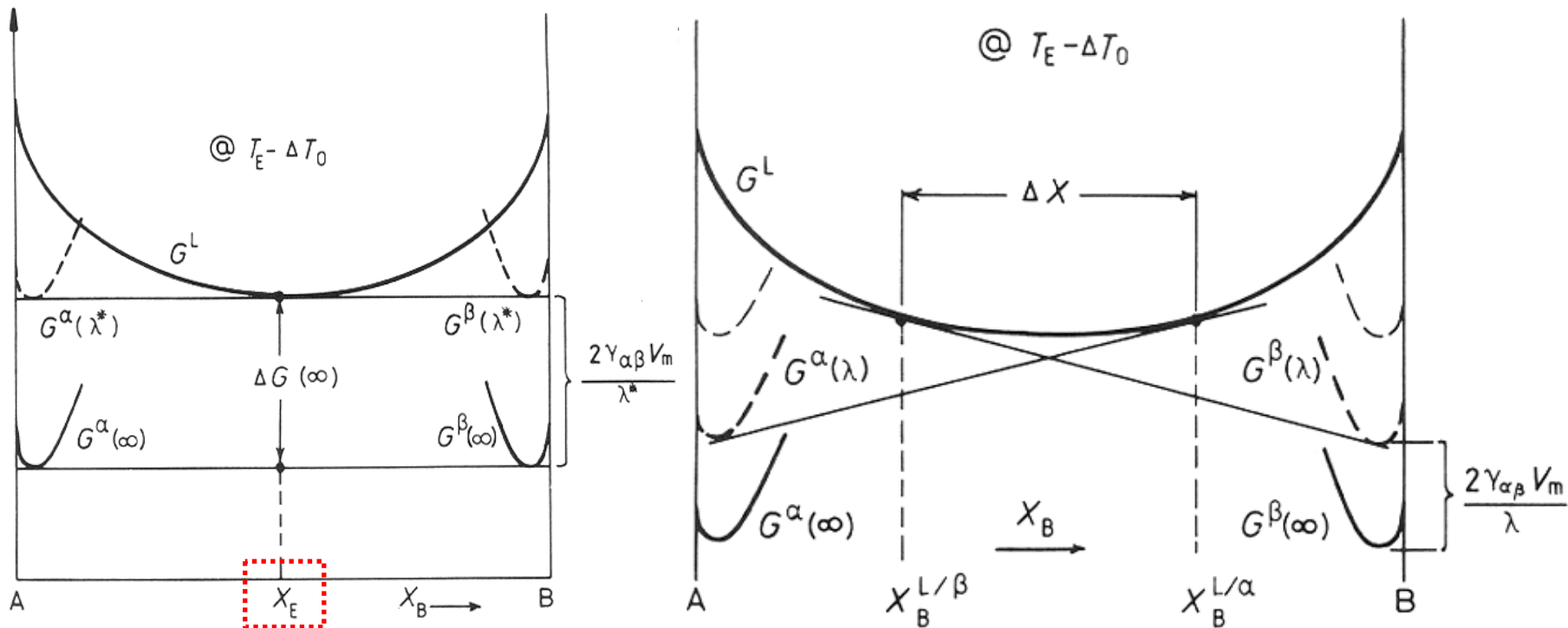
$$\text{cf) } r^* = \frac{2\gamma_{SL}}{\Delta G_V} = \left(\frac{2\gamma_{SL} T_m}{L_V} \right) \frac{1}{\Delta T}$$

L_V : latent heat per unit volume

$$L = \Delta H = H^L - H^S$$

$$\lambda^* = -\frac{2T_E \gamma V_m}{\Delta H \Delta T_0} \rightarrow \text{identical to critical radius}$$

Gibbs-Thomson effect in a ΔG -composition diagram?



β 상과 국부적
평형 이루는
액상의 조성 < α 상과 국부적
평형 이루는
액상의 조성

공정의 성장속도 v

→ 액상을 통한 용질이동과 비례

→ 성장 확산 제어

$$v \propto D \frac{dC}{dl} \propto (X_B^{L/\alpha} - X_B^{L/\beta})$$

$\propto 1/\text{유효확산거리} \dots 1/\lambda$

$$v = k_1 D \frac{\Delta X}{\lambda}$$

$$\lambda = \lambda^*, \Delta X = 0$$

$$\lambda = \infty, \Delta X = \Delta X_0$$

$$\Delta X = \Delta X_0 \left(1 - \frac{\lambda^*}{\lambda}\right)$$

$$\Delta X_0 \propto \Delta T_0$$

$$v = k_2 D \frac{\Delta T_0}{\lambda} \left(1 - \frac{\lambda^*}{\lambda}\right)$$

Maximum growth rate at a fixed $\Delta T_0 \rightarrow \lambda = 2\lambda^*$

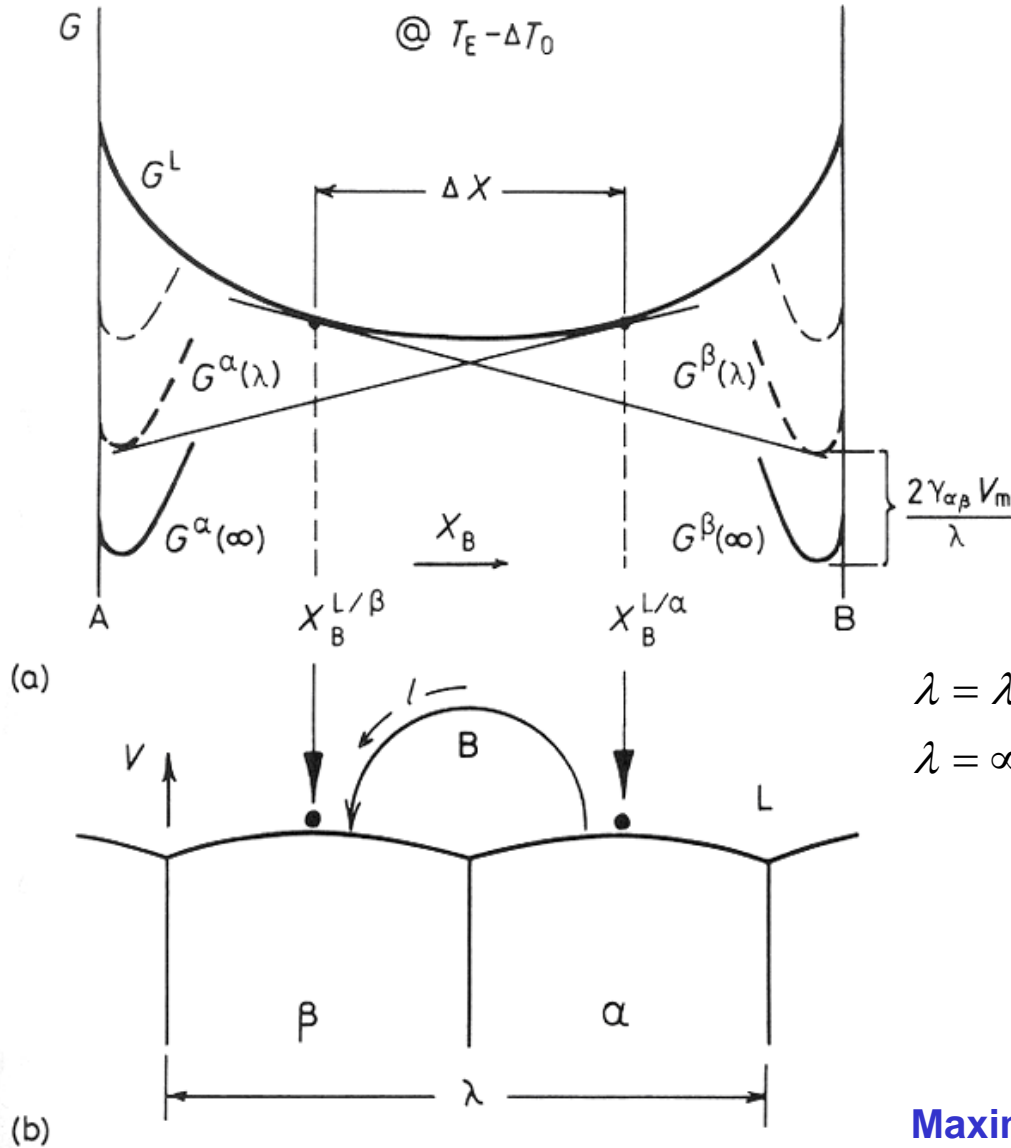


Fig. 4.33 (a) Molar free energy diagram at $(T_E - \Delta T_0)$ for the case $\lambda^* < \lambda < \infty$, showing the composition difference available to drive diffusion through the liquid (ΔX). (b) Model used to calculate the growth rate.

Corresponding location at phase diagram?

$$\Delta T_0 = \Delta T_r + \Delta T_D$$

$$\Delta G_{total} = \Delta G_r + \Delta G_D$$

$$\Delta G_r = \frac{2\gamma_{\alpha\beta} V_m}{\lambda}$$

→ free energy dissipated in forming α/β interfaces

ΔG_D → free energy dissipated in diffusion

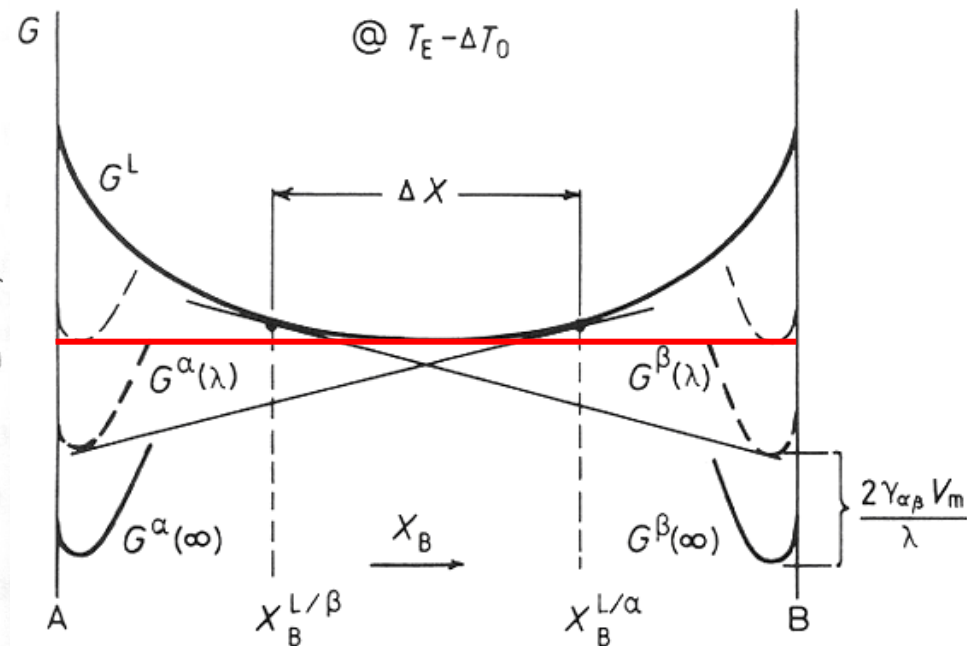
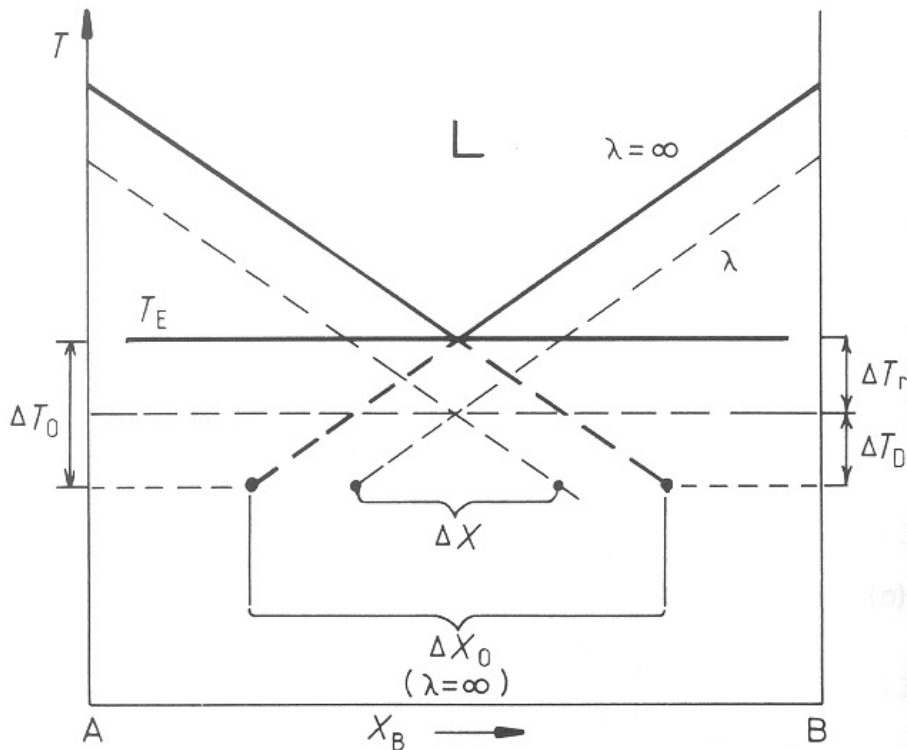


Fig. 4.34 Eutectic phase diagram showing the relationship between ΔX and ΔX_0 (exaggerated for clarity)

$$v = k_2 D \frac{\Delta T_0}{\lambda} \left(1 - \frac{\lambda^*}{\lambda}\right)$$

Maximum growth rate at a fixed $\Delta T_0 \rightarrow \lambda = 2\lambda^*$

$$v_0 = k_2 D \Delta T_0 / 4\lambda^*$$

$$\lambda^* = -\frac{2T_E \gamma V_m}{\Delta H \Delta T_0} \text{로부터, } \Delta T_0 \propto 1/\lambda^*$$

$\lambda = \lambda_0$ 인 경우,

$$v_0 \lambda_0^2 = k_3$$

$$\frac{v_0}{(\Delta T_0)^2} = k_4$$

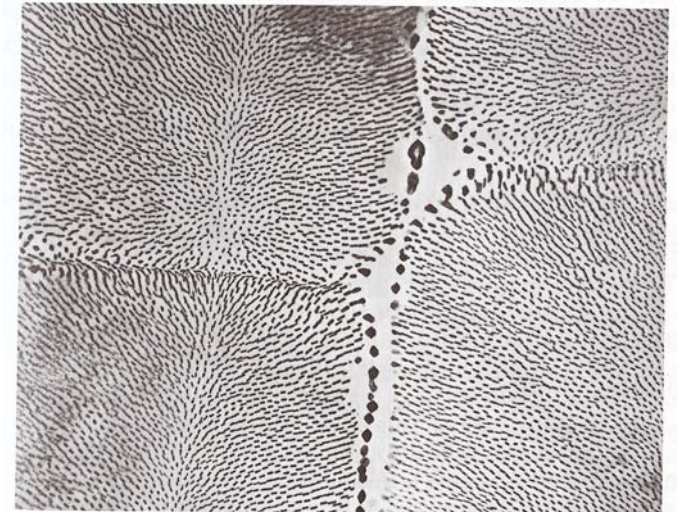
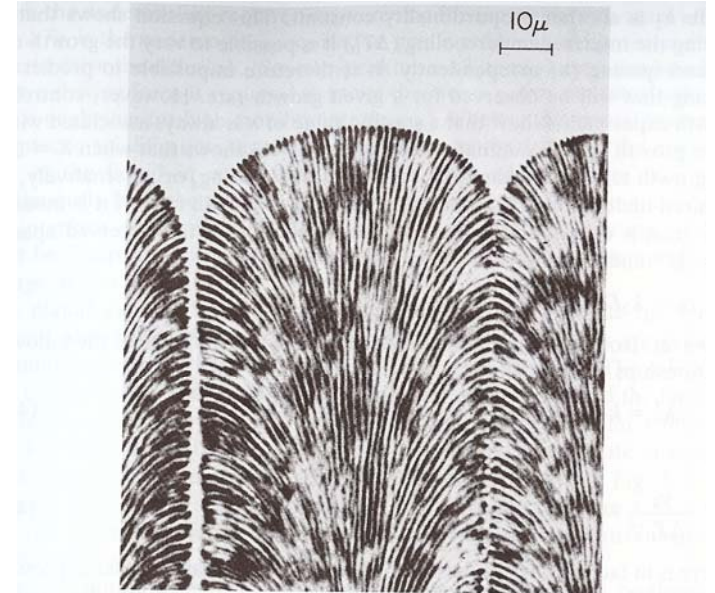
$$\Delta T_0 = \Delta T_r + \Delta T_D$$

계면 곡률효과 확산위해 충분한 조
극복 과냉도 성차주기 위한 과냉

$\Delta T_D \rightarrow \alpha$ 층의 중간부터 β 층의 중간까지 변화

$\Delta T_0 = 0$ 계면 등은 항상 등은

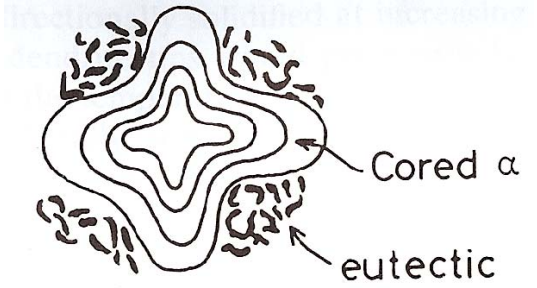
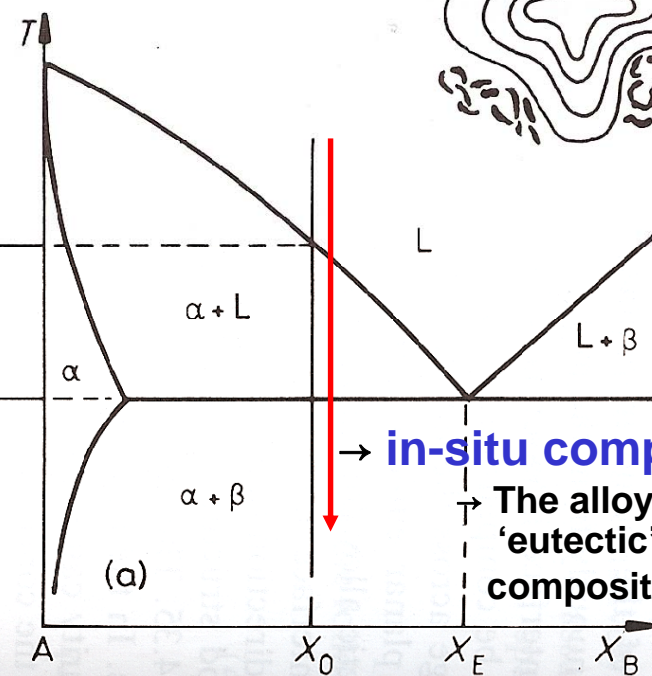
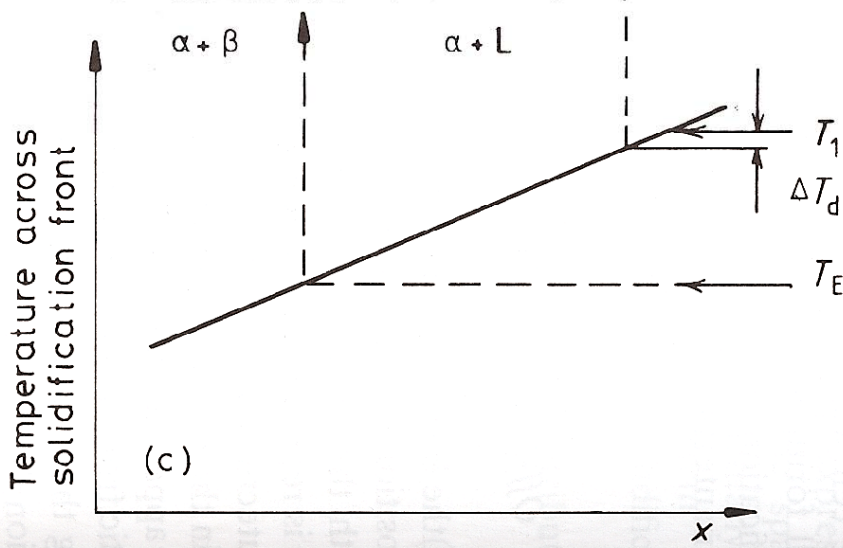
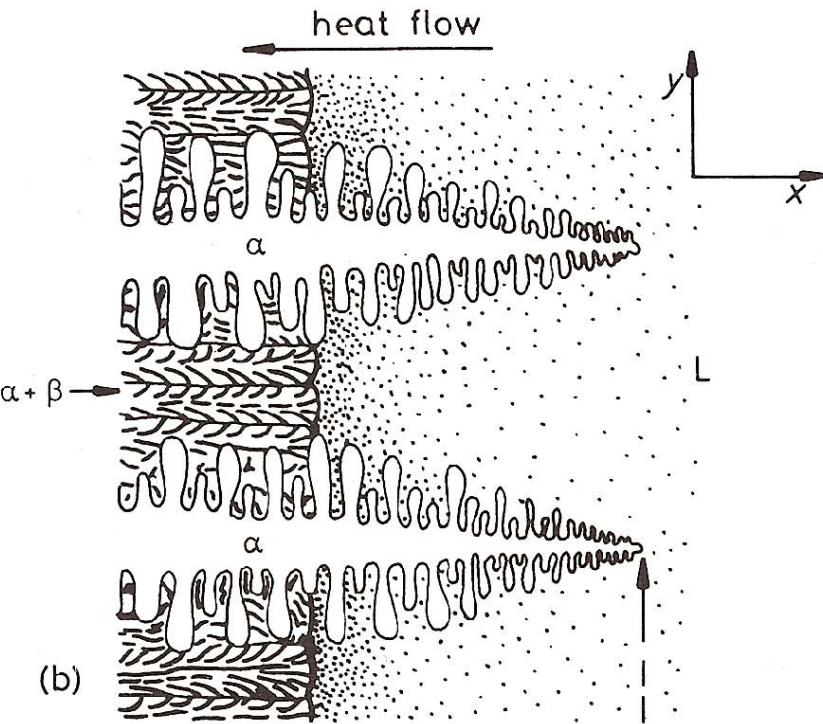
ΔT_r 로 극복해야 함 \rightarrow 계면의 곡률을 따라 변화



4.3.3 Off-eutectic Solidification

proeutectic α + eutectic lamellar

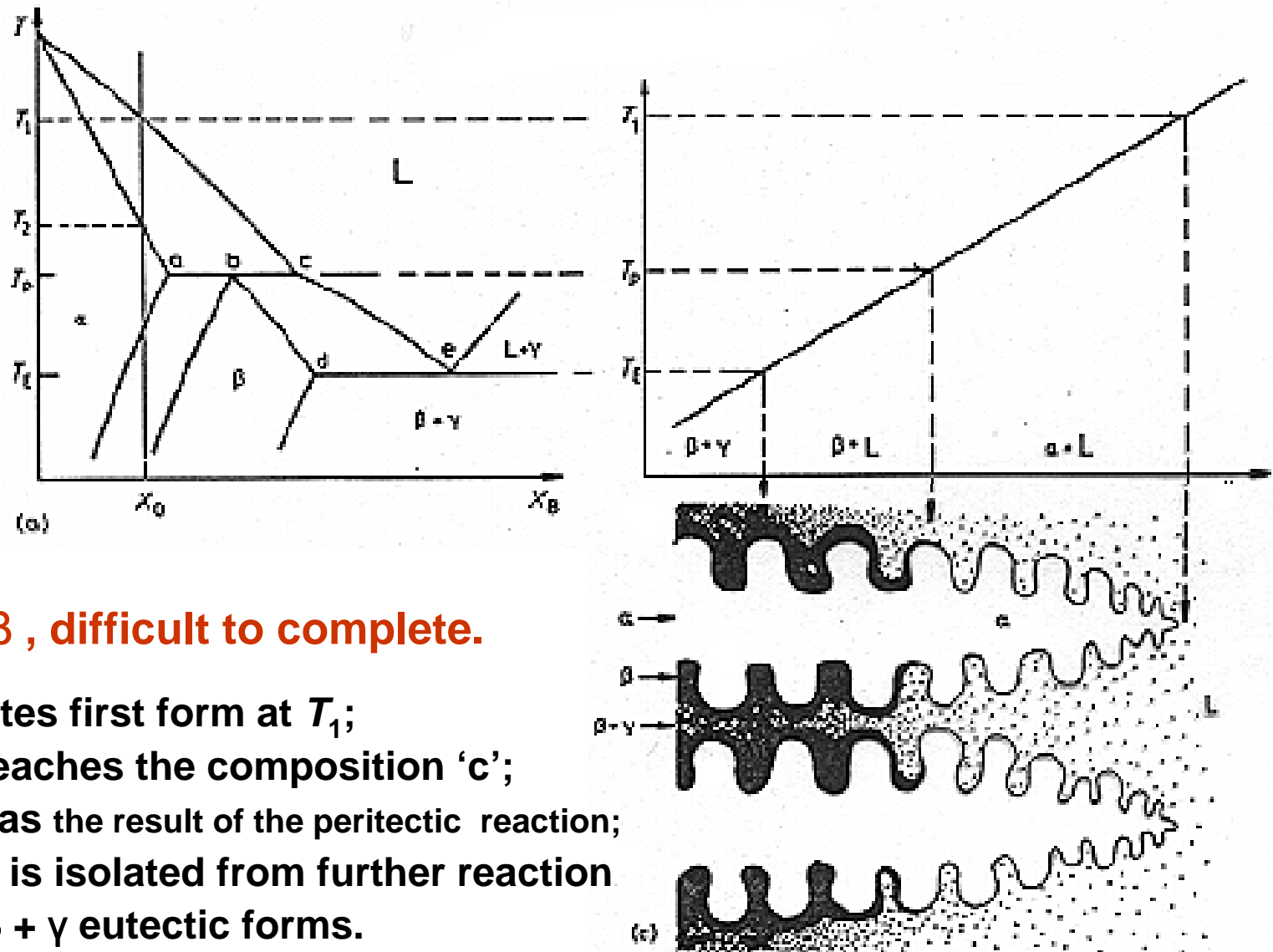
- Primary α dendrites form at T_1 . Rejected solute increases X_L to X_E ; eutectic solidification follows.
- **Coring**: primary α (low solute) at T_1 and the eutectic (high solute) at T_E .



in-situ composite materials

The alloy solidifies as 100% 'eutectic' with an overall composition X_0 instead of X_E .

4.3.4 Peritectic Solidification



- $L + \alpha \rightarrow \beta$, difficult to complete.
- α dendrites first form at T_1 ;
Liquid reaches the composition 'c';
 β forms as the result of the peritectic reaction;
 α coring is isolated from further reaction
finally $\beta + \gamma$ eutectic forms.

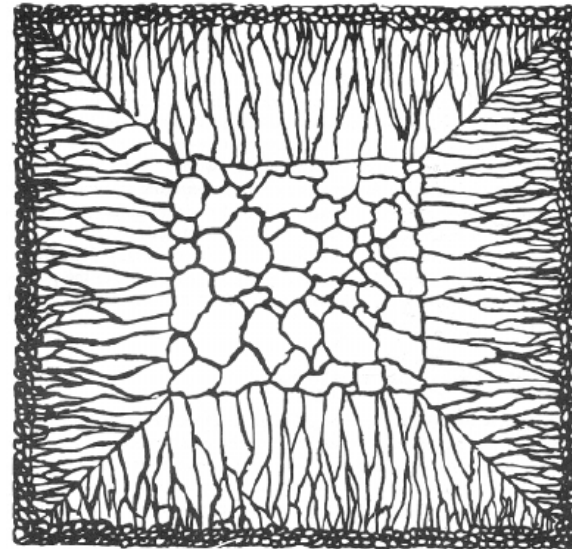
4.4 Solidification of Ingots and Castings

주조 후 압연, 압출 또는 단조 등에 의해 가공된 것 >> blank (작은 것)

주조된 제품이 최종 모양을 유지하거나 혹은 기계가공에 의해 최종 모양으로 된 것

Ingot Structure

- Chill zone
- Columnar zone
- Equiaxed zone



Chill zone

- Solid nuclei form on the mould wall and begin to grow into the liquid.
- As the mould wall warms up it is possible for many of these solidified crystals to break away from the wall under the influence of the turbulent melt.

Columnar zone

After pouring the **temperature gradient** at the mould walls **decreases** and the crystals in the chill zone grow dendritically in certain crystallographic directions, e.g. **<100>** in the case of cubic metals.

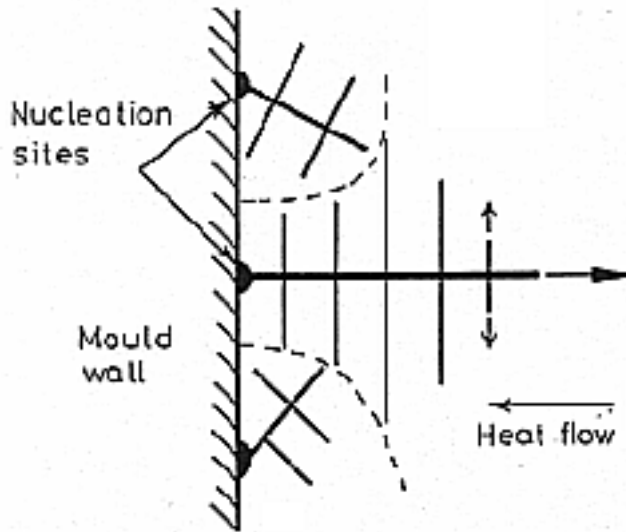


Fig. 4.41 Competitive growth soon after pouring. Dendrites with primary arms normal to the mould wall, i.e. parallel to the maximum temperature gradient, outgrow less favorably oriented neighbors.

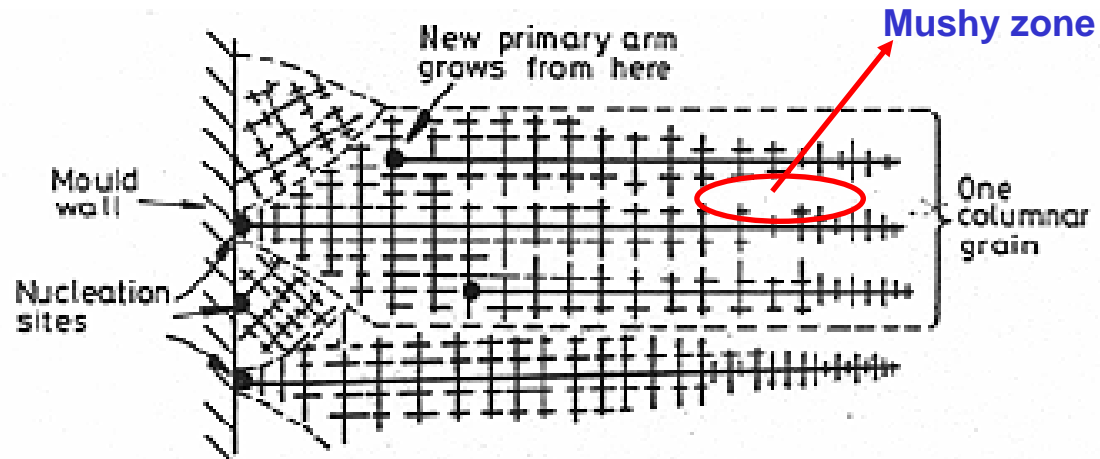
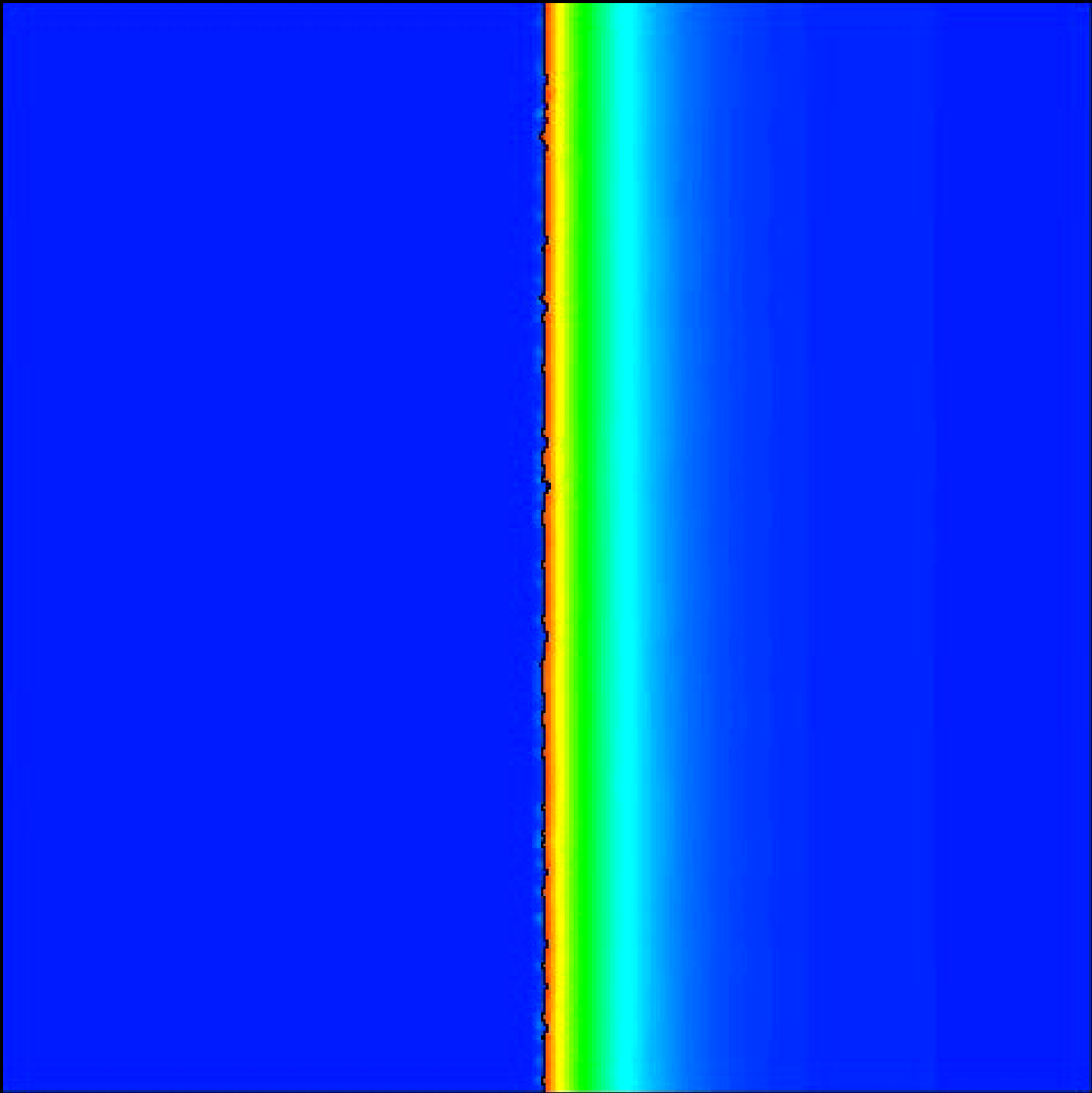


Fig. 4.42 Favorably oriented dendrites develop into columnar grains. Each columnar grain originates from the same heterogeneous nucleation site, but can contain many primary dendrite arms.



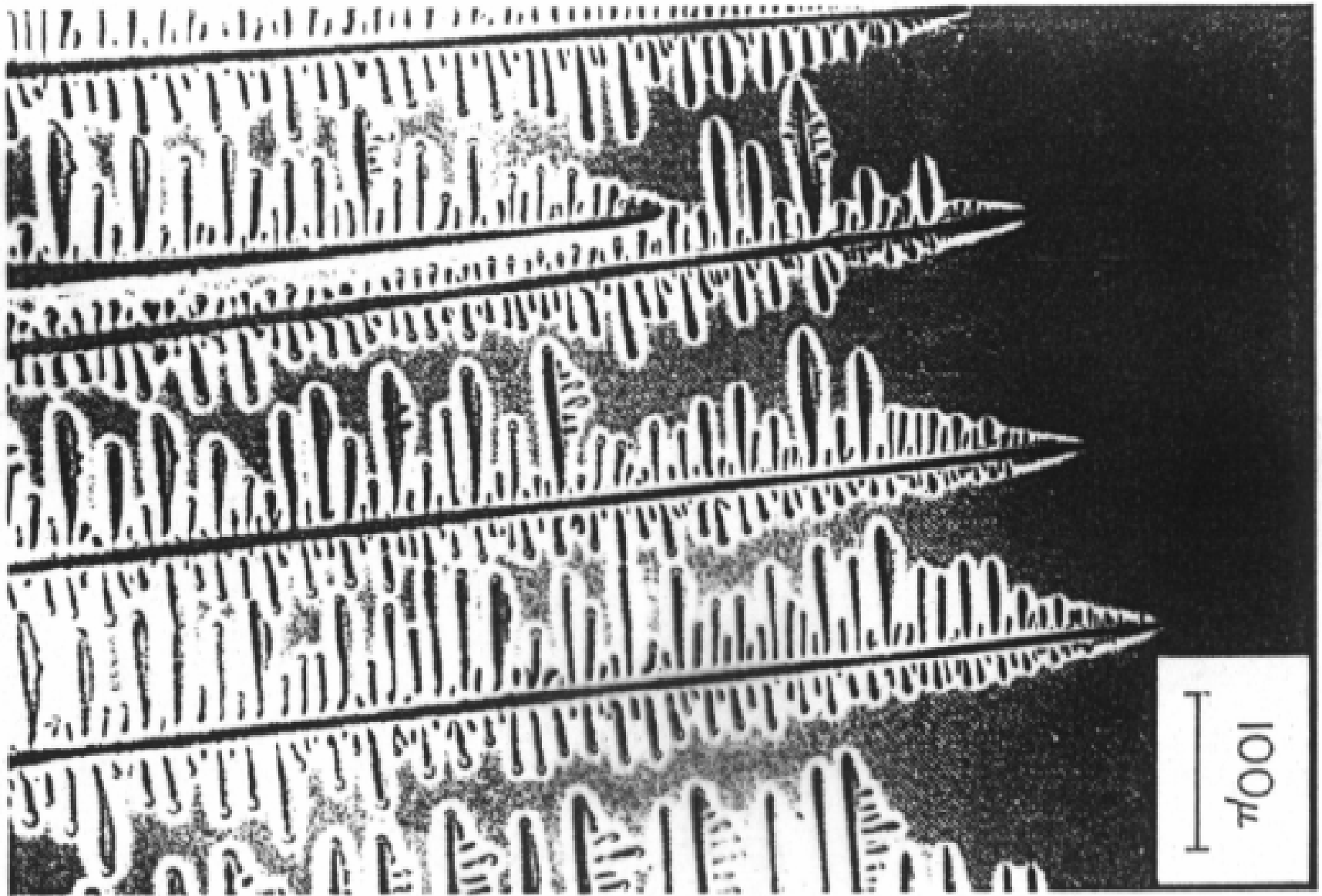


Fig. 4.28 Columnar dendrites in a transparent organic alloy.
(After K.A. Jackson in *Solidification*, American Society for Metals, 1971, p. 121.)³⁰

Equiaxed zone

The equiaxed zone consists of **equiaxed grains randomly** oriented in the centre of the ingot. An important origin of these grains is thought to be **melted-off dendrite side-arms**. + **convection current**

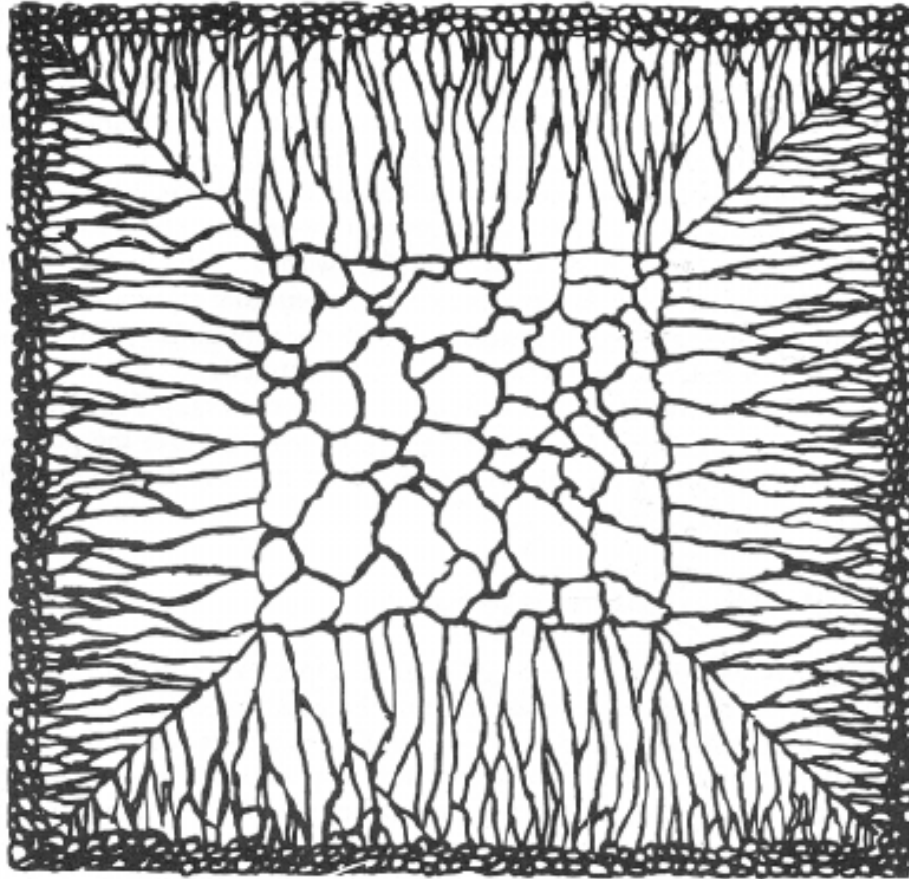
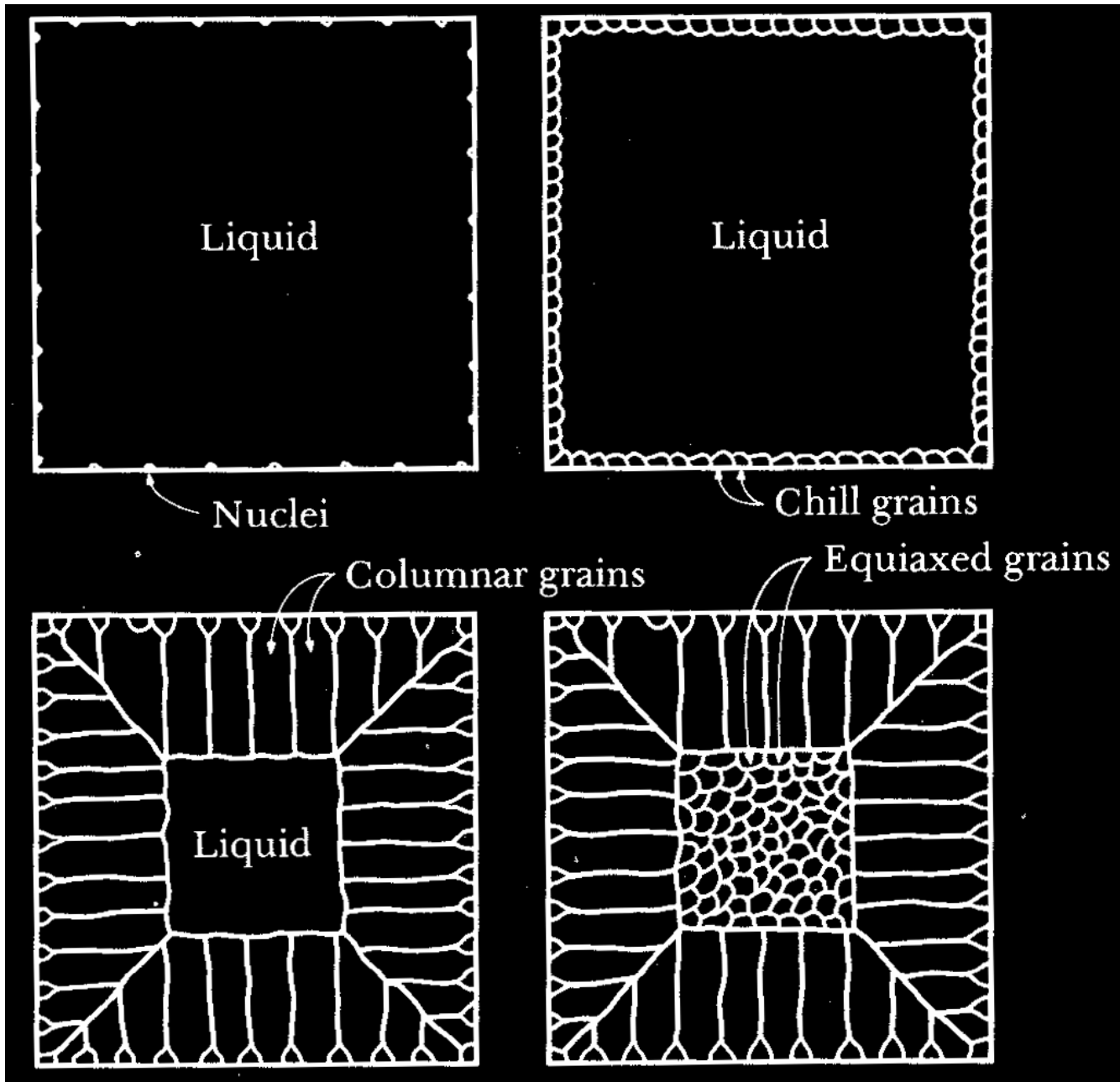


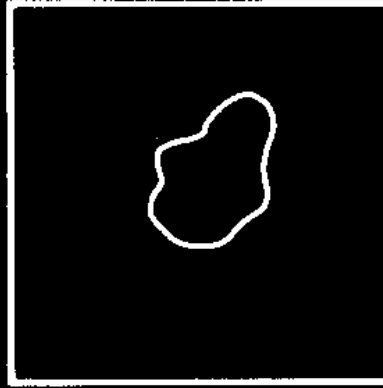
Fig. 4.40 Schematic cast grain structure.

(After M.C. Flemings, Solidification Processing, McGraw-Hill, New York, 1974.) ³¹

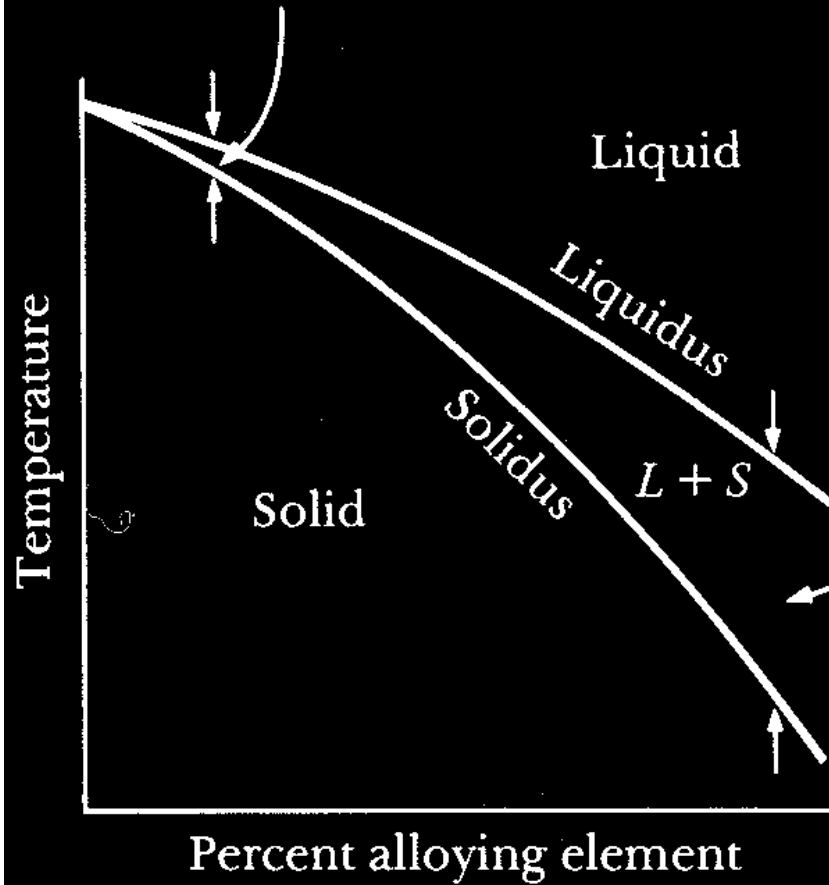
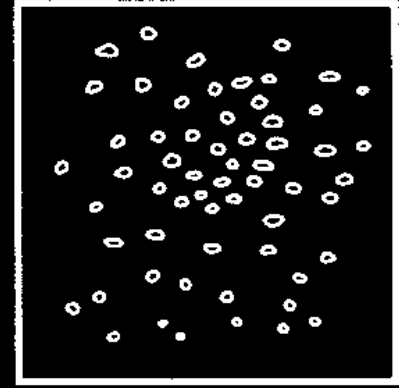


Shrinkage effect

Narrow freezing range



Wide freezing range

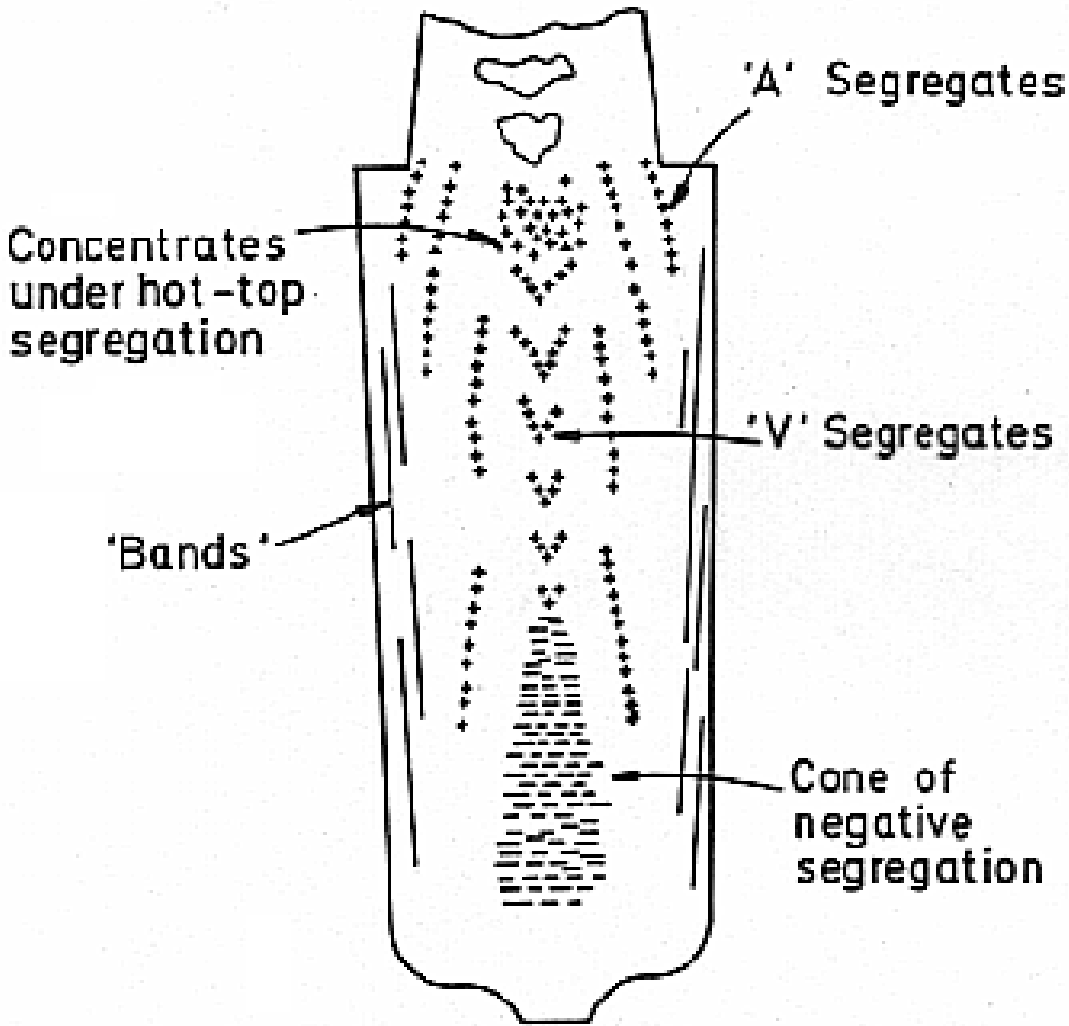


4.4.2 Segregation in Ingots and Castings

- **Macrosegregation** :
Composition changes over distances comparable to the size of the specimen.
- **Microsegregation** :
Occur on the scale of the secondary dendrite arm spacing.

Four important factors that can lead to macrosegregation

- **Shrinkage due to solidification and thermal contraction.**
- **Density differences in the interdendritic liquid.**
- **Density differences between the solid and liquid**
- **Convection currents driven by temperature-induced density differences in the liquid.**

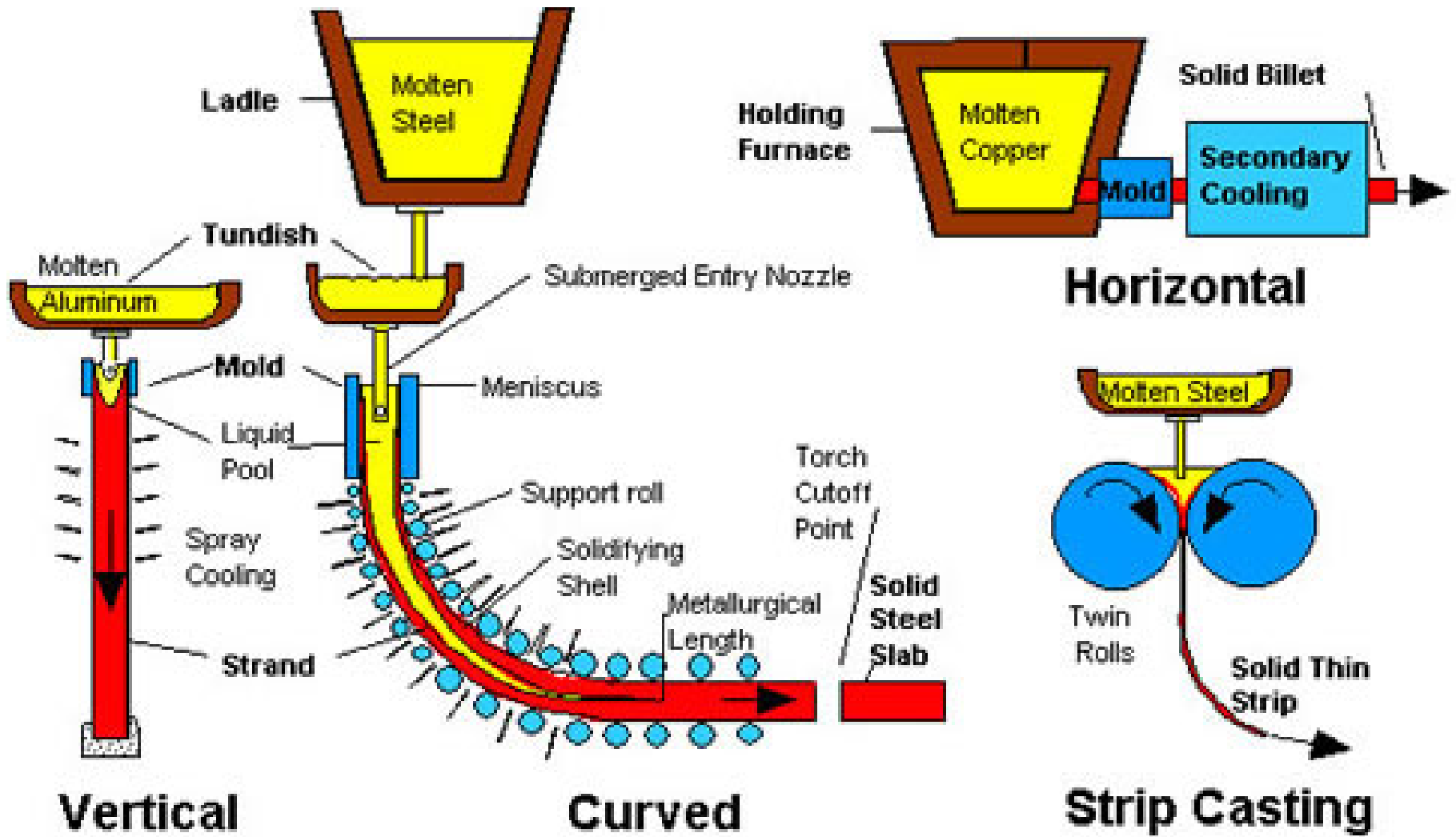


역편석: 주상정 수지상이 두꺼워지면 용질이 농축된 액상 ($k < 1$ 인 경우)이 수축을 보충하기 위해 수지상 사이로 다시 흘러들어온다.

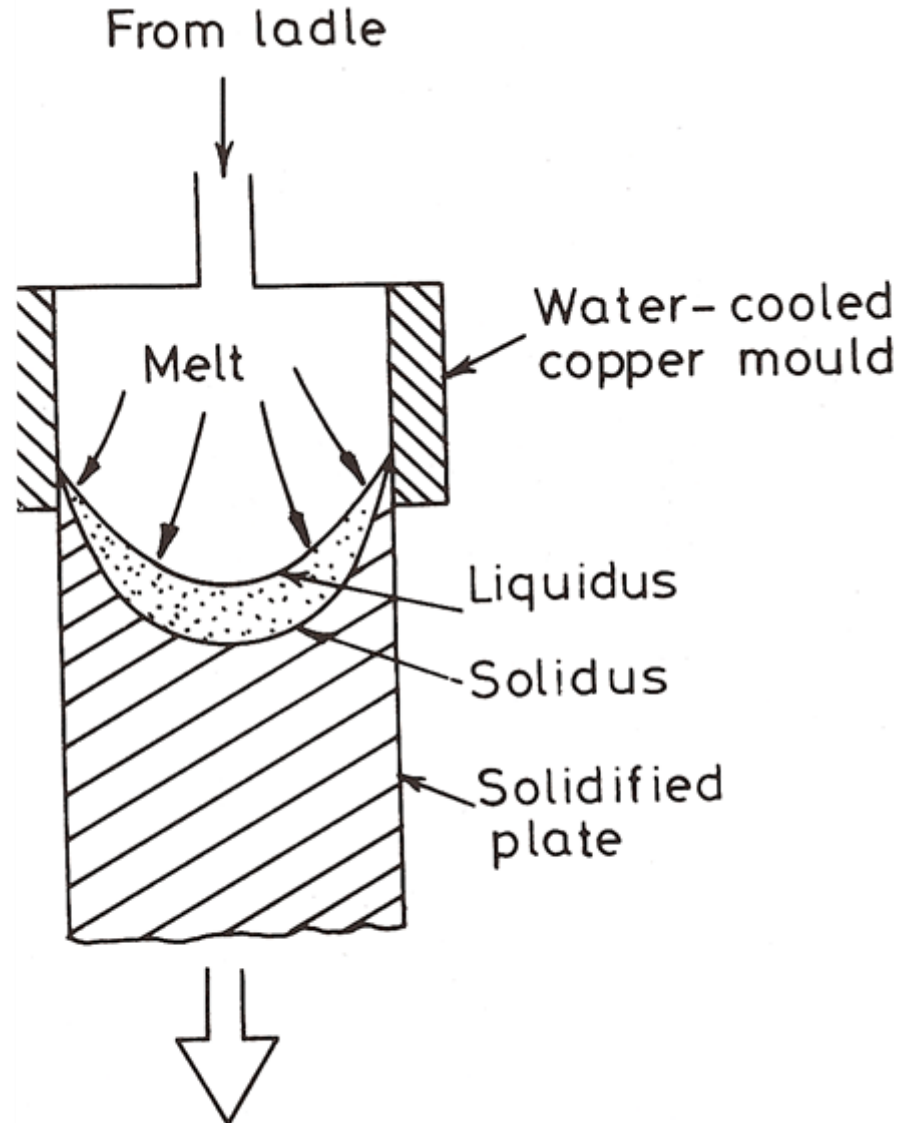
음의 편석: 등축결정 형성시 중력효과에 의함. 일반적으로 고상은 액상보다 밀도 높고, $k < 1$ 이라면 고상의 조성은 본래의 조성보다 낮은 조성을 가짐.

Fig. 4.43 Segregation pattern in a large killed steel ingot. + positive, - negative segregation. (After M.C. Flemings, Scandinavian Journal of Metallurgy 5 (1976) 1.)

4.4.3 continuous casting



4.4.3 continuous casting

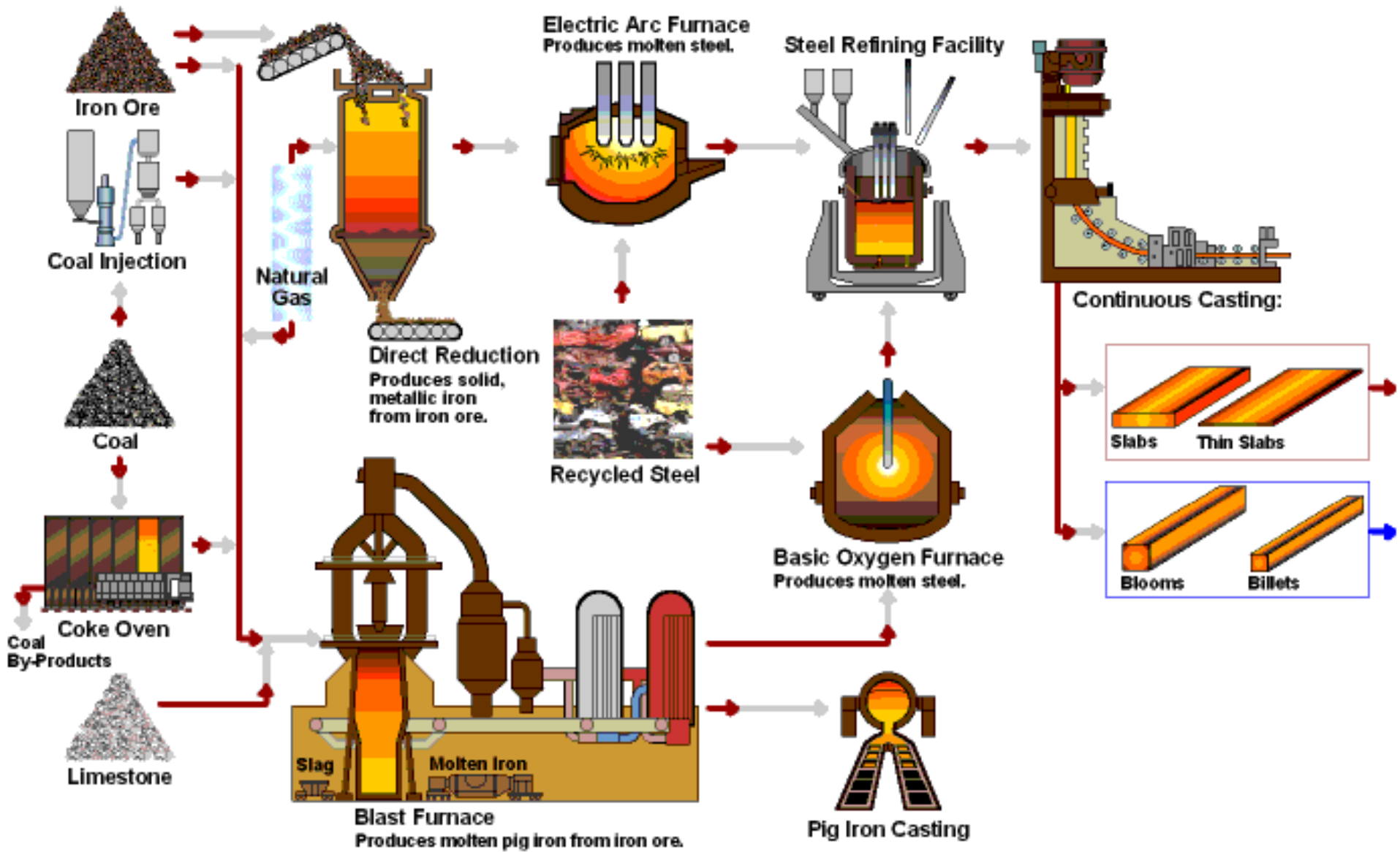


Schematic illustration of a continuous casting process.

4.4.3 continuous casting



4.4.3 continuous casting



4.4.3 continuous casting

